HIGGS PHYSICS AND ELECTROWEAK SYMMETRY BREAKING*

Peter M. Zerwas

Deutsches Elektronen-Synchrotron DESY
D-22603 Hamburg, Germany

(Received April 1, 1999)

Higgs physics at prospective e^+e^- linear colliders is reviewed in the context of the Standard Model and supersymmetric theories. A brief overview is also given on strong interactions of the electroweak bosons at TeV energies in alternative scenarios.

PACS numbers: 12.15.–y, 14.80.Bn, 14.80.Cp

1. Introduction

1. Revealing the physical mechanism which breaks the electroweak symmetries, is one of the key problems in particle physics. If the standard particles — leptons, quarks and gauge bosons — remain weakly interacting up to very high energies, the sector in which the electroweak symmetries are broken must contain one or more fundamental scalar Higgs bosons with light masses of the order of the symmetry breaking scale $v = [\sqrt{2}G_{\rm F}]^{-1/2} \sim 246$ GeV. The masses of the fundamental particles are generated by the interactions with the scalar background Higgs field, being non-zero in the ground state [1]. Alternatively, the symmetry breaking could be generated dynamically by new strong forces characterized by an interaction scale $\Lambda \sim 1$ TeV [2]. If global symmetries of these strong interactions are broken spontaneously, the associated Goldstone bosons can be absorbed by the gauge fields, generating the longitudinal degrees of freedom and the masses of the gauge particles. The masses of leptons and quarks can be generated by interactions with the fermion condensate, mediated by extended gauge interactions.

2. A simple mechanism for the breaking of the electroweak symmetries is incorporated in the Standard Model (SM) [3]. To accommodate all observed phenomena, an isodoublet scalar field is introduced which, by self-interactions, acquires a non-vanishing vacuum expectation value, breaking

* Presented at the Cracow Epiphany Conference on Electron–Positron Colliders, Cracow, Poland, January 5–10, 1999.

spontaneously the electroweak symmetries $\mathrm{SU}(2)_I\times$ $\mathrm{U}(1)_Y$ symmetry. The interactions of the gauge bosons and fermions with the background field generate the masses of these particles. One scalar field component is not absorbed in this process, manifesting itself as the physical Higgs particle H.

The mass of the Higgs boson is the only unknown parameter in the symmetry breaking sector of the Standard Model while the couplings are fixed by the masses of the particles, a consequence of the Higgs mechanism *sui generis*. However, the mass of the Higgs boson is strongly constrained. Since the quartic self-coupling of the Higgs field grows indefinitely with rising energy, an upper limit on the Higgs mass can be derived by demanding the SM particles to remain weakly interacting up to a scale Λ [4]. On the other hand, stringent lower bounds on the Higgs mass follow from requiring the electroweak vacuum to be stable [5]. If the Standard Model is valid up to scales near the Planck scale, the SM Higgs mass is restricted to a narrow window between 130 and 190 GeV. For Higgs masses either above or below this window, new interactions are expected to occur at a scale Λ between ~ 1 TeV and the Planck scale [4, 6].

The electroweak observables are affected by the Higgs mass through radiative corrections [7]. Despite of the weak logarithmic dependence, the high-precision electroweak data indicate a preference for light Higgs masses close to ~ 100 GeV [8]. At 95% CL, the data require a value of the Higgs mass less than about 250 GeV. By searching directly for the SM Higgs particle, the LEP experiments have set a lower limit of about 90 to 95 GeV on the Higgs mass [9]. If the Higgs boson will not be found at LEP2, the search will continue at the Tevatron. The proton collider LHC can sweep the entire canonical Higgs mass range of the Standard Model. The properties of the Higgs particle can subsequently be analyzed very accurately at e^+e^- linear colliders [10]. By measuring the couplings of the Higgs boson to gauge particles, leptons and quarks, and by reconstructing the self-interaction of the Higgs field, essential elements of the Higgs mechanism can be established experimentally.

3. If the Standard Model is embedded in a Grand Unified Theory (GUT) at high energies, the natural scale of the electroweak symmetry breaking would be expected close to the unification scale M_{GUT}. Supersymmetry [11] provides a solution of this hierarchy problem. The quadratically divergent contributions to the radiative corrections of the scalar Higgs boson mass are cancelled by the destructive interference between supersymmetrized bosonic and fermionic loops [12]. A strong indication for the realization of this physical picture in Nature is the excellent agreement between the value of the electroweak mixing angle $\sin^2\theta_W$ predicted by the unification of the gauge couplings, and the measured value. If the gauge couplings are unified in the minimal supersymmetric theory at a scale $M_{\mathrm{GUT}} = \mathcal{O}(10^{16}$ GeV), the electroweak mixing angle is predicted to be $\sin^2\theta_W = 0.2336 \pm 0.0017$ [13] for a mass spectrum of the supersymmetric particles of order M_Z to 1 TeV. This theoretical prediction must be compared with the experimental result $\sin^2\theta_W^{\rm exp} = 0.2316 \pm 0.0003$ [8]; the difference of the two numbers is less than 2 per mille.

In the Minimal Supersymmetric extension of the Standard Model (MSSM), the Higgs sector is built up by two Higgs doublets [14]. The doubling is necessary to generate masses for up- and down-type fermions in a supersymmetric theory and to render the theory anomaly-free. The Higgs particle spectrum consists of a quintet of states: two $\mathcal{CP}$-even scalar neutral (h, H), one $\mathcal{CP}$-odd pseudoscalar neutral (A), and a pair of charged $(H^\pm)$ Higgs bosons [15]. The masses of the heavy Higgs bosons, $H, A, H^\pm$, are expected to be of order v but may extend up to the TeV range. By contrast, since the quartic Higgs self-couplings are determined by the gauge couplings, the mass of the lightest Higgs boson h is constrained very stringently. At tree-level, the mass has been predicted to be smaller than the Z mass [15]. Radiative corrections, increasing as the fourth power of the top mass, shift the upper limit to a value between ~ 100 GeV and ~ 130 GeV, depending on the mixing parameter $\tan\beta$.

A general lower bound of 73 GeV has been established for the Higgs particle h experimentally at LEP [9]. Continuing this search, the entire h mass range can be covered for $\tan\beta \lesssim 2$, one of two areas predicted by the unification of the b and τ masses at high energies. The search for h masses in excess of ~ 100 GeV and the search for the heavy Higgs bosons will continue at the Tevatron, the LHC and e^+e^- linear colliders. In these machines the mass range up to ~ 1 TeV can be covered [10].

4. Elastic scattering amplitudes of longitudinally polarized massive vector bosons grow indefinitely with energy if they are calculated as a perturbative expansion in the coupling of a non-abelian gauge theory. As a result they violate unitarity beyond a critical energy scale of ~ 1.2 TeV. This problem can be solved by introducing a light Higgs boson. In alternative scenarios, the W bosons may become strongly interacting at TeV energies, thus damping the rise of the elastic scattering amplitudes. Naturally, the strong forces between the W bosons may be traced back to new fundamental interactions characterized by a scale of order 1 TeV [2]. If the underlying theory is globally chiral-invariant, the symmetry may be broken spontaneously. The Goldstone bosons associated with the spontaneous symmetry breaking can be absorbed by the gauge bosons to build up the longitudinal degrees of freedom of the wave functions and to generate their masses.

Since the longitudinally polarized W bosons are associated with the Goldstone modes, the scattering amplitudes of the $W_{\rm L}$ bosons can be predicted for high energies by a systematic expansion in the energy. The leading term is parameter-free, a consequence of the chiral symmetry breaking mechanism *per se* which is independent of the particular dynamical theory.

Such a scenario can be studied in WW scattering experiments with W bosons radiated, as quasi-real particles [16], off the electron and positron beams in TeV linear colliders [10, 17, 18].

5. This report is divided into three parts. A basic summary of the main theoretical and experimental results expected from e^+e^- linear colliders will be presented in the next section on the Higgs sector of the Standard Model. The Higgs spectrum of supersymmetric theories will be discussed in the subsequent section. Finally, the main features of strong W interactions and their analysis in WW scattering experiments will be presented in the last section.

Only the basic elements of electroweak symmetry breaking and the Higgs mechanism can be described in this report. Other aspects may be traced back from Ref. [19] and recent review reports collected in Ref. [20].

2. The Higgs sector of the Standard Model

2.1. The basis of the Higgs mechanism

For high energies, the amplitude for elastic scattering of massive W bosons, $WW \to WW$, grows indefinitely with energy for longitudinally polarized particles. Even though the term of the amplitude rising as the fourth power in the energy is cancelled by virtue of the non-abelian gauge symmetry, the amplitude remains quadratically divergent in the energy. On the other hand, unitarity requires elastic scattering amplitudes of partial waves J to be bounded by $\Re e A_J \leq 1/2$. Applied to the asymptotic S-wave amplitude $A_0 = G_{\rm F} s/8\pi\sqrt{2}$ of the isospin-zero channel $2W_{\rm L}^+ W_{\rm L}^- + Z_{\rm L} Z_{\rm L}$, with $\sqrt{s}$ denoting the cm energy, the bound on the energy [21]

$$s \leq 4\pi\sqrt{2}/G_{\rm F} \sim (1.2 \text{ TeV})^2, \tag{1}$$

can be derived for the validity of a theory of weakly coupled massive gauge bosons.

However, the quadratic rise in the energy can be damped by exchanging a scalar particle. To achieve the cancellation, the size of the coupling must be given by the product of the gauge coupling with the gauge boson mass. For high energies, the amplitude $A_0' = -G_{\rm F} s/8\pi\sqrt{2}$ cancels exactly the quadratic divergence of the pure gauge boson amplitude A_0. Thus, unitarity can be restored by introducing a weakly coupled fundamental *Higgs particle*.

In the same way, the linear divergence of the amplitude $A(f\bar{f} \to W_L W_L) \sim g m_f \sqrt{s}$ for the annihilation of a fermion–antifermion pair to a pair of longitudinally polarized gauge bosons can be damped by adding the Higgs exchange to the gauge boson exchange. In this case the Higgs particle must couple proportional to the mass m_f of the fermion f.

These observations can be summarized in a theorem: *A theory of massive gauge bosons and fermions which are weakly coupled up to very high energies, requires, by unitarity, the existence of a Higgs particle; the Higgs particle is a scalar 0^+ particle which couples to other particles proportional to the masses of the particles.*

The assumption that the couplings of the fundamental particles are weak up to very high energies, is qualitatively supported by the perturbative renormalization of the electroweak mixing angle $\sin^2\theta_W$ from the symmetry value $3/8$ at the GUT scale down to ~ 0.2 which is close to the experimentally observed value at low energies.

These ideas can be cast into an elegant mathematical form by interpreting the electroweak interactions as a gauge theory with spontaneous symmetry breaking in the scalar sector. Such a theory consists of fermion fields, gauge fields and a scalar field coupled by the standard gauge interactions and Yukawa interactions to the other fields. Moreover, a quartic self-interaction

$$V = \frac{\lambda}{2}\left[|\phi|^2 - \frac{v^2}{2}\right]^2 \tag{2}$$

is introduced in the scalar sector which gives rise to a non-zero ground-state value $v/\sqrt{2}$ of the scalar field. By fixing the phase of the vacuum amplitude to zero, the electroweak symmetries are spontaneously broken in the scalar sector. Interactions of the gauge fields with the scalar background field and Yukawa interactions of the fermion fields with the background field shift the masses of these fields from zero to non-zero values:

$$\begin{aligned}
&\text{(a)} \quad \frac{1}{q^2} \to \frac{1}{q^2} + \sum_j \frac{1}{q^2}\left[\left(\frac{gv}{\sqrt{2}}\right)^2 \frac{1}{q^2}\right]^j = \frac{1}{q^2 - M^2}: \quad M^2 = g^2\frac{v^2}{2}, \\
&\text{(b)} \quad \frac{1}{\not{q}} \to \frac{1}{\not{q}} + \sum_j \frac{1}{\not{q}}\left[\frac{g_f v}{\sqrt{2}}\frac{1}{\not{q}}\right]^j = \frac{1}{\not{q} - m_f}: \qquad m_f = g_f\frac{v}{\sqrt{2}}.
\end{aligned} \tag{3}$$

Thus in theories with gauge and Yukawa interactions, in which the scalar field acquires a non-zero ground-state value, the couplings are naturally proportional to the masses. This ensures the unitarity of the theory.

In the electroweak $SU_2 \times U_1$ Lagrangean the scalar isodoublet field ϕ is coupled to the gauge fields by the covariant derivative $iD = i\partial - g\vec{I}\vec{W} - g'YB$, and to the up and down fermion fields u, d by Yukawa interactions:

$$\mathcal{L}_0 = |D\phi|^2 - \frac{\lambda}{2}\left[|\phi|^2 - \frac{v^2}{2}\right]^2 - g_d \bar{d}_\mathrm{L}\phi d_\mathrm{R} - g_u \bar{u}_\mathrm{L}\phi_c u_\mathrm{R} + \mathrm{h.c.} \qquad (4)$$

In the unitary gauge, the isodoublet ϕ is replaced by the physical Higgs field H, $\phi \to [0, (v+H)/\sqrt{2}]$, which describes the deviation of the $I_3 = -1/2$ component of the isodoublet field from the ground state value $v/\sqrt{2}$. The quartic coupling λ and the Yukawa couplings g_f can be reexpressed in terms of the physical Higgs mass M_H and the fermion masses m_f, $M_H^2 = \lambda v^2$ and $m_f = g_f v/\sqrt{2}$, respectively.

Since the couplings of the Higgs particle to gauge particles, fermions and to itself are given by the gauge couplings and the masses of the particles, the only unknown parameter in the Higgs sector is the Higgs mass. When this mass is fixed, all properties of the Higgs particle can be predicted, *i.e.* the lifetime and decay branching ratios, as well as the production mechanisms and the corresponding cross sections.

2.1.1. The SM Higgs mass

Stringent upper and lower bounds on the mass of the Higgs boson can be derived in the Standard Model, from internal consistency conditions and extrapolations of the model to high energies.

The Higgs boson has been introduced as a fundamental particle to render 2–2 scattering amplitudes involving longitudinally polarized W bosons compatible with unitarity. Based on the general principle of time-energy uncertainty, particles must decouple from a physical system if their mass grows indefinitely. The mass of the Higgs particle must therefore be bound to restore unitarity in the perturbative regime. From the asymptotic expansion of the elastic $W_\mathrm{L}W_\mathrm{L}$ S-wave scattering amplitude including W and Higgs exchanges, $A(W_\mathrm{L}W_\mathrm{L} \to W_\mathrm{L}W_\mathrm{L}) \to -G_\mathrm{F}M_H^2/4\sqrt{2}\pi$, it follows [21] that the Higgs mass must be bound by

$$M_H^2 \leq 2\sqrt{2}\pi/G_\mathrm{F} \sim (850\ \mathrm{GeV})^2. \qquad (5)$$

Within the canonical formulation of the Standard Model, consistency conditions therefore require a Higgs mass below 1 TeV.

Very restrictive bounds on the value of the SM Higgs mass follow from hypotheses on the energy scale Λ up to which the Standard Model can be extended before new strong interactions between the fundamental particles become effective. The key to these bounds is the evolution of the quartic coupling λ with the energy (*i.e.* the field strength) due to quantum fluctuations [4]. The Higgs loop itself gives rise to an indefinite increase of the coupling while the fermionic top-quark loop drives, with increasing top mass, the coupling to smaller values, eventually even to values below zero. The variation of the quartic Higgs coupling λ and of the top-Higgs Yukawa coupling g_t with energy, parametrized by $t = \log \mu^2/v^2$, may be written as [4]

$$\begin{aligned} \frac{d\lambda}{dt} &= \frac{3}{8\pi^2}\left[\lambda^2 + \lambda g_t^2 - g_t^4\right] : \quad \lambda(v^2) = \frac{M_H^2}{v^2}\,, \\ \frac{dg_t}{dt} &= \frac{1}{32\pi^2}\left[\frac{9}{2}g_t^3 - 8 g_t g_s^2\right] : \quad g_t(v^2) = \sqrt{2}\frac{m_f}{v} \end{aligned} \tag{6}$$

taking into account only the leading contributions from H, t and QCD loops.

For moderate top masses, the quartic coupling λ rises indefinitely, $\dot{\lambda} \sim +\lambda^2$, and the coupling becomes strong shortly before reaching the Landau pole at

$$\lambda(\mu^2) = \frac{\lambda(v^2)}{\left[1 - \frac{3\lambda(v^2)}{8\pi^2}\log\frac{\mu^2}{v^2}\right]}\,.$$

Reexpressing the initial value of λ by the Higgs mass, the condition $\lambda(\Lambda) < \infty$, can be translated to an *upper bound* on the Higgs mass:

$$M_H^2 \leq \frac{8\pi^2 v^2}{3\log\frac{\Lambda^2}{v^2}}\,. \tag{7}$$

This mass bound is related logarithmically to the energy Λ up to which the Standard Model is assumed to be valid. The maximal value of M_H for the minimal cut-off $\Lambda \sim 1$ TeV is given by ~ 750 GeV.

A *lower bound* on the Higgs mass can be derived from the requirement of vacuum stability [4, 5]. Since top-loop corrections decrease λ for increasing top-Yukawa coupling, λ becomes negative if the top mass becomes too large. In this case, the self-energy potential would become deep negative and the ground state would not be stable any more. To avoid the instability, the Higgs mass must balance the drop by exceeding a minimal value for a given top mass. This lower bound depends on the cut-off value Λ.

For any given Λ the allowed values of (M_t, M_H) pairs are shown in Fig. 1. For a central top mass $M_t = 175$ GeV, the Higgs mass values are collected in Table I for two specific cut-off values Λ. If the Standard Model is assumed to be valid up to the scale of grand unification, the Higgs mass is restricted to a narrow window between 130 and 190 GeV. The observation of a Higgs mass above or below this window would demand a new physics scale below the GUT scale.

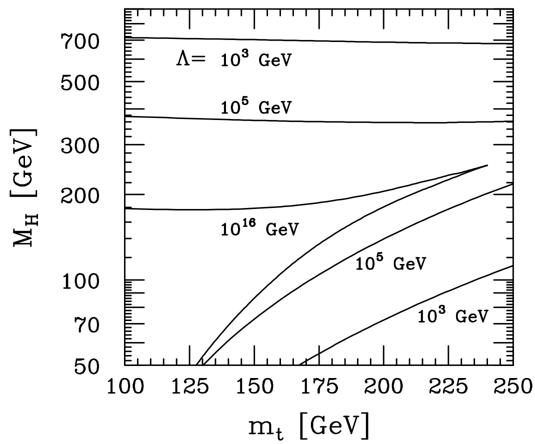

Fig. 1. Bounds on the mass of the Higgs boson in the SM. Λ denotes the energy scale at which the Higgs-boson system of the SM would become strongly interacting (upper bound); the lower bound follows from the requirement of vacuum stability. Refs [4, 5].

TABLE I

Higgs mass bounds for two values of the cut-off Λ

Λ	M_H
1 TeV	55 GeV $\lesssim M_H \lesssim$ 700 GeV
10^{16} GeV	130 GeV $\lesssim M_H \lesssim$ 190 GeV

2.1.2. Decays of the Higgs particle

The profile of the Higgs particle is uniquely determined if the Higgs mass is fixed. The strength of the Yukawa couplings of the Higgs boson to fermions is set by the fermion masses m_f, and the coupling to the electroweak gauge bosons $V = W, Z$ by their masses M_V:

$$\begin{aligned} g_{Hff} &= \left[\sqrt{2}G_{\mathrm{F}}\right]^{1/2} m_f \, , \\ g_{HVV} &= 2\left[\sqrt{2}G_{\mathrm{F}}\right]^{1/2} M_V^2 \, . \end{aligned} \tag{8}$$

The total decay width and lifetime, as well as the branching ratios for specific decay channels are determined by these parameters. The measurement of the decay characteristics can therefore be exploited to establish experimentally that Higgs couplings grow with the masses of the particles.

The partial width of Higgs decays to lepton and quark pairs is given by [22]

$$\Gamma(H \to f\bar{f}) = \mathcal{N}_c \frac{G_{\rm F}}{4\sqrt{2}\pi} m_f^2(M_H^2) M_H \,. \tag{9}$$

$\mathcal{N}_c = 1$ or 3 is the color factor. Near threshold the partial width is suppressed by an additional factor β_f^3 where β_f is the fermion velocity. Asymptotically, the fermionic width grows linearly with the Higgs mass. The bulk of the QCD radiative corrections can be mapped into the scale dependence of the quark mass, evaluated at the Higgs mass. For $M_H \sim 100$ GeV the relevant parameters are $m_b(M_H^2) \simeq 3$ GeV and $m_c(M_H^2) \simeq 0.6$ GeV. The reduction of the effective c-quark mass overcompensates the color factor in the ratio between charm and τ decays of Higgs bosons.

Above the WW and ZZ decay thresholds, the partial widths for these channels may be written as [23]

$$\Gamma(H \to VV) = \delta_V \frac{G_{\rm F}}{16\sqrt{2}\pi} M_H^3 (1 - 4x + 12x^2)\beta_V \,, \tag{10}$$

where $x = M_V^2/M_H^2$ and $\delta_V = 2$ and 1 for $V = W$ and Z, respectively. For large Higgs masses, the vector bosons are longitudinally polarized. Since the wave-functions of these states are linear in the energy, the widths grow as the third power of the Higgs mass. Below the threshold for two real bosons, the Higgs particle can decay into VV^* pairs, one of the vector bosons being virtual [24].

In the Standard Model, gluonic Higgs decays are mediated by top- and bottom-quark loops, photonic decays in addition by W loops. Since these decay modes are significant only far below the top and W thresholds, they can be described by the approximate expressions [25, 26]

$$\Gamma(H \to gg) \;=\; \frac{G_{\rm F}\alpha_s^2}{36\sqrt{2}\pi^3} M_H^3 \left[1 + \left(\frac{95}{4} - \frac{7N_{\rm F}}{6}\right)\frac{\alpha_s}{\pi}\right] , \tag{11}$$

$$\Gamma(H \to \gamma\gamma) \;=\; \frac{G_{\rm F}\alpha^2}{128\sqrt{2}\pi^3} M_H^3 \left|\frac{4}{3}\mathcal{N}_C e_t^2 - 7\right|^2 \tag{12}$$

which are valid in the limit $M_H^2 \ll 4M_W^2, 4M_t^2$. The QCD radiative corrections which include ggg and $gq\bar{q}$ final states in (11), are very important; they increase the partial width by about 65%. Even though photonic Higgs decays are very rare, they nevertheless offer a simple and attractive signature for Higgs particles by leading just to two stable quanta in the final state.

By adding up all possible decay channels, we obtain the total width: Up to masses of 140 GeV, the Higgs particle is very narrow, $\Gamma(H) \leq 10$ MeV. After opening up the real and virtual gauge boson channels, the state becomes rapidly wider, reaching a width of ~ 1 GeV at the ZZ threshold. The width cannot be measured directly in the intermediate mass region at the LHC or e^+e^- colliders; it could be measured at muon colliders in the lower part of the intermediate range [27]. Above ~ 250 GeV, the state becomes wide enough to be resolved experimentally in general. Since the width grows as the third power of the mass, the Higgs particle becomes very wide, $\Gamma(H) \sim \frac{1}{2} M_H^3$ [TeV], for high masses. In fact, for $M_H \sim 1$ TeV, the width reaches $\sim \frac{1}{2}$ TeV.

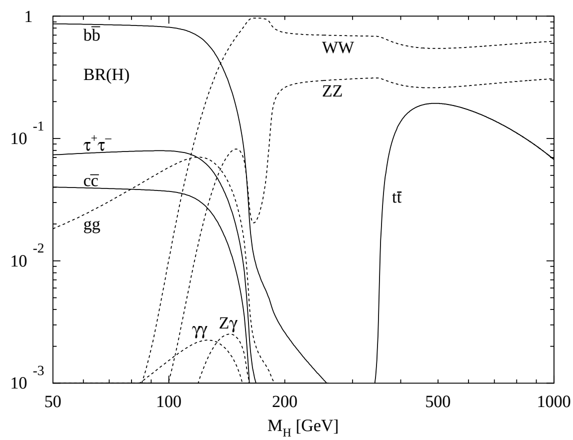

Fig. 2. Branching ratios of the dominant decay modes of the SM Higgs particle. All relevant higher order corrections are taken into account.

The branching ratios of the main decay modes are displayed in Fig. 2. A large variety of channels will be accessible for Higgs masses below 140 GeV. The dominant mode are $b\bar{b}$ decays, yet $c\bar{c}, \tau^+\tau^-$ and gg still occur at a level of several per cent. $\gamma\gamma$ decays occur at a level of 1 per mille. Above ~ 140 GeV, the Higgs boson decay into W's becomes dominant, overwhelming all other channels if the decay mode into two real W's is kinematically possible. For Higgs masses far above the thresholds, ZZ and WW decays occur at a ratio of $1:2$, slightly modified only just above the $t\bar{t}$ threshold.

2.2. Electroweak precision data: Higgs-mass estimate

Strong indirect evidence for a light Higgs boson can be derived from the high-precision measurements of electroweak observables at LEP and elsewhere. Indeed, the fact that the Standard Model is renormalizable only after including the top and Higgs particles in the loop corrections, indicates that the electroweak observables are sensitive to the masses of these particles.

The Fermi coupling can be rewritten in terms of the weak coupling and the W mass:

$$\frac{G_{\mathrm{F}}}{\sqrt{2}} = \frac{2\pi\alpha}{\sin^2 2\theta_W M_Z^2}[1 + \Delta r_\alpha + \Delta r_t + \Delta r_H]\,. \tag{13}$$

The Δ terms take account of the radiative corrections. Δr_α describes the shift in the electromagnetic coupling if evaluated at the scale M_Z^2 instead of zero-momentum. Δr_t denotes the top (and bottom) quark contribution to the W mass which is quadratic in the top mass. Finally, Δr_H accounts for the virtual Higgs contributions to the masses; this term depends only logarithmically [7] on the Higgs mass at leading order,

$$\Delta r_H = \frac{G_{\mathrm{F}} M_W^2}{8\sqrt{2}\pi^2}\frac{11}{3}\left[\log\frac{M_H^2}{M_W^2} - \frac{5}{6}\right], \qquad (M_H^2 \gg M_W^2)\,. \tag{14}$$

The screening effect reflects the role of the Higgs field as a regulator which renders the electroweak theory renormalizable.

Although the sensitivity on the Higgs mass is only logarithmic, the increasing precision in the measurement of the electroweak observables allow us to derive interesting estimates and constraints on the Higgs mass:

$$\begin{aligned} M_H &= 98^{+77}_{-45}\ \mathrm{GeV} \\ &< 240\ \mathrm{GeV} \qquad (95\%\ \mathrm{CL})\,. \end{aligned} \tag{15}$$

It may be concluded from these numbers that a light Higgs boson in the canonical formulation of the Standard Model is nicely compatible with the high-precision electroweak data. However, alternative scenarios including strong interactions that are not under proper theoretical control, cannot be ruled out by these indirect analyses.

Future e^+e^- linear colliders are planned to operate at low energies near the W^+W^- threshold and on the Z boson with very high luminosity, generating more than 1 GigaZ events. The accuracy in $\sin^2\vartheta_W$ and M_W measurements is expected to improve by an order of magnitude compared to the present errors: $\delta\sin^2\vartheta_W \sim 0.00002$ and $\delta M_W \sim 6$ MeV. Based on these measurements the Higgs mass can be determined within $\Delta M_H/M_H \sim 10\%$. Assuming that the Higgs particle will have been discovered at that time, the indirect measurement provides an important theoretical test of the underlying field theory which incorporates the spontaneous breaking of the electroweak gauge symmetries.

2.3. Higgs production channels at e^+e^- colliders

The two main production mechanisms for Higgs bosons in e^+e^- collisions are the processes

$$\text{Higgs-strahlung} : e^+e^- \to Z^* \to ZH\,, \tag{16}$$

$$WW \text{ fusion} : e^+e^- \to \bar{\nu}_e\nu_e(WW) \to \bar{\nu}_e\nu_e H\,. \tag{17}$$

In Higgs-strahlung [26, 28, 29] the Higgs boson is emitted from the Z-boson line while WW-fusion is a formation process of Higgs bosons in the collision of two quasi-real W bosons radiated off the electron and positron beams [30].

As evident from the subsequent analyses, LEP2 can cover the SM Higgs mass range up to about 100 GeV. The high energy e^+e^- linear colliders can cover the entire Higgs mass range in the second phase in which they will reach a total energy of about 2 TeV [10]. For an integrated luminosity of $\int\mathcal{L} = 1\text{ab}^{-1}$, more than 10^5 Higgs boson events are generated, the majority of which accompanied by charged leptons and neutrinos and little contaminated by backgrounds.

2.3.1. Higgs-strahlung

The cross section for Higgs-strahlung can be written in a compact form,

$$\sigma(e^+e^- \to ZH) = \frac{G_F^2 M_Z^4}{96\pi s}\left[v_e^2 + a_e^2\right]\lambda^{1/2}\frac{\lambda + 12M_Z^2/s}{\left[1 - M_Z^2/s\right]^2}, \tag{18}$$

where v_e and a_e are the vector and axial-vector Z charges of the electron and λ is the usual two-particle phase space function. The cross section is of the size $\sigma \sim \alpha_w^2/s$, *i.e.* of second order in the weak coupling, and it scales in the squared energy.

Since the cross section vanishes for asymptotic energies, the Higgs-strahlung process is most useful for searching Higgs bosons in the range where the collider energy is of the same order as the Higgs mass, $\sqrt{s} \gtrsim \mathcal{O}(M_H)$. The size of the cross section is illustrated in Fig. 3 for the energies $\sqrt{s} = 500$ and 800 GeV of e^+e^- linear colliders as a function of the Higgs mass. Since the recoiling Z mass in the two-body reaction $e^+e^- \to ZH$ is mono-energetic, the mass of the Higgs boson can be reconstructed from the energy of the Z boson, $M_H^2 = s - 2\sqrt{s}E_Z + M_Z^2$, without any need of analyzing the decay products of the Higgs boson. For leptonic Z decays, missing mass techniques provide a very clear signal as demonstrated in Fig. 4.

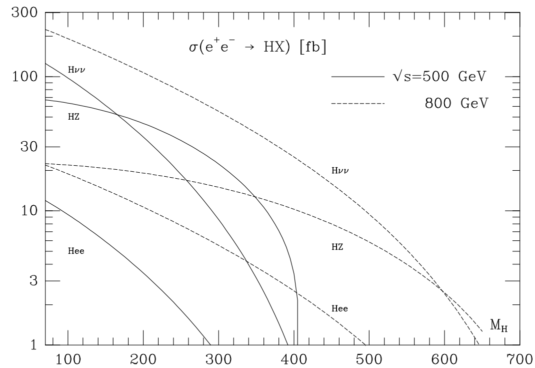

Fig. 3. The cross section for the production of SM Higgs bosons in Higgs-strahlung $e^+e^- \to ZH$ and WW/ZZ fusion $e^+e^- \to \bar{\nu}_e\nu_e/e^+e^-H$; solid curves: $\sqrt{s} = 500$ GeV, dashed curves: $\sqrt{s} = 800$ GeV.

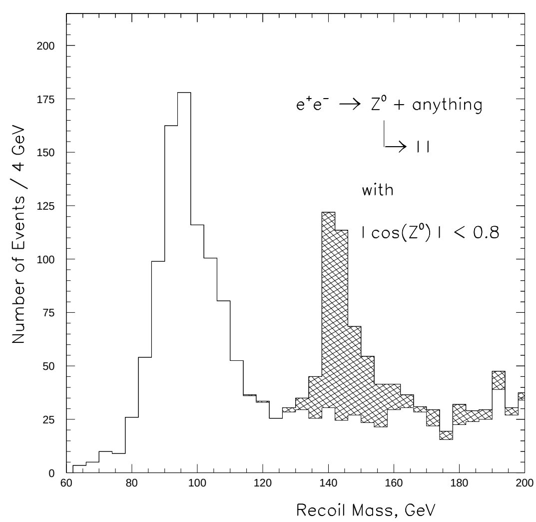

Fig. 4. Dilepton recoil mass analysis of Higgs-strahlung $e^+e^- \to ZH \to \ell^+\ell^-+$ anything in the intermediate Higgs mass range for $M_H = 140$ GeV. The c.m. energy is $\sqrt{s} = 360$ GeV and the integrated luminosity $\int \mathcal{L} = 50\text{fb}^{-1}$. Ref. [31].

2.3.2. *WW* fusion

Also the cross section for the fusion process (17) can be cast implicitly into a compact form,

$$\sigma(e^+e^- \to \bar{\nu}_e\nu_e H) = \frac{G_F^3 M_W^4}{4\sqrt{2}\pi^3} \int_{\kappa_H}^{1} \int_{x}^{1} \frac{dx\ dy}{[1+(y-x)/\kappa_W]^2} f(x,y)\,, \tag{19}$$

$$f(x,y) = \left(\frac{2x}{y^3} - \frac{1+3x}{y^2} + \frac{2+x}{y} - 1\right)\left[\frac{z}{1+z} - \log(1+z)\right] + \frac{x}{y^3}\frac{z^2(1-y)}{1+z}$$

with $\kappa_H = M_H^2/s$, $\kappa_W = M_W^2/s$ and $z = y(x-\kappa_H)/(\kappa_W x)$.

Since the fusion process is a t-channel exchange process, the size is set by the W Compton wave length, suppressed however with respect to Higgs-strahlung by the third power of the electroweak coupling, $\sigma \sim \alpha_w^3/M_W^2$. As a result, W fusion becomes the leading production process for Higgs particles at high energies. At asymptotic energies the cross section simplifies to

$$\sigma(e^+e^- \to \bar{\nu}_e\nu_e H) \to \frac{G_{\rm F}^3 M_W^4}{4\sqrt{2}\pi^3}\left[\log\frac{s}{M_H^2} - 2\right]. \tag{20}$$

In this limit, W fusion to Higgs bosons can be interpreted as a two-step process: The $W^\pm$ bosons are radiated as quasi-real particles from electrons and positrons, $e^\pm \to \overset{(-)}{\nu_e} W^\pm$, with the Higgs bosons generated subsequently in the colliding W beams: $W^+W^- \to H$.

The size of the fusion cross section is compared with Higgs-strahlung in Fig. 3. At $\sqrt{s} = 500$ GeV the two cross sections are of the same order, yet the fusion process becomes increasingly important with rising energy.

2.3.3. $\gamma\gamma$ fusion

The production of Higgs bosons in $\gamma\gamma$ collisions [32] can be exploited to determine important properties of these particles, in particular the two–photon decay width. The $H\gamma\gamma$ coupling is built up by loops of charged particles. If the mass of the loop particle is generated by the Higgs mechanism, the decoupling of the heavy particles is switched off and the $\gamma\gamma$ width reflects the spectrum of these states with masses possibly far above the Higgs mass.

The two-photon width is related to the production cross section for polarized γ beams by

$$\sigma(\gamma\gamma \to H) = \frac{16\pi^2 \Gamma(H\to\gamma\gamma)}{M_H} \times \mathrm{BW}, \tag{21}$$

where BW denotes the Breit–Wigner resonance factor in terms of the energy squared. For narrow Higgs bosons the observed cross section is found by folding the parton cross section with the invariant $\gamma\gamma$ flux $d\mathcal{L}^{\gamma\gamma}/d\tau$ for $J_z^{\gamma\gamma} = 0$ at $\tau = M_H^2/s_{ee}$.

The event rate for the production of Higgs bosons in $\gamma\gamma$ collisions of Weizsäcker–Williams photons is too small to play a role in practice. However, the rate is sufficiently large if the photon spectra are generated by Compton back-scattering of laser light. The $\gamma\gamma$ invariant energy in such a Compton collider [33] is of the same size as the parent e^+e^- energy and the luminosity is expected to be suppressed only by one order of magnitude compared with the luminosity in e^+e^- collisions. In the Higgs mass range between 100 and 150 GeV, the final state consists primarily of $b\bar{b}$ pairs. The large $\gamma\gamma$ continuum background is suppressed in the $J_z^{\gamma\gamma} = 0$ polarization state. For Higgs masses above 150 GeV, WW final states become dominant, supplemented in the ratio 1 : 2 by ZZ final states above the ZZ decay threshold. While the continuum WW background in $\gamma\gamma$ collisions is very large, the ZZ background appears under control for masses up to order 300 GeV [32].

2.4. The profile of the Higgs particle

To establish the Higgs mechanism experimentally, the nature of the particle must be explored by measuring all its characteristics, the mass and lifetime, the external quantum numbers spin-parity, the couplings to gauge bosons and fermions, and last but not least, the Higgs self-couplings.

2.4.1. Mass

The mass of the Higgs particle can be measured by collecting the decay products of the particle. In e^+e^- collisions Higgs-strahlung can be exploited to reconstruct the mass very precisely from the Z recoil energy in the two-body process $e^+e^- \to ZH$, as discussed already before. An overall accuracy of about $\delta M_H \sim 50$ MeV can be expected at high luminosity.

2.4.2. Width/lifetime

The width of the state, *i.e.* the lifetime of the particle, can be measured directly above the ZZ decay threshold where the width grows rapidly. In the lower part of the intermediate mass range the width can be measured indirectly by combining the branching ratio for $H \to \gamma\gamma$, accessible in the chain $e^+e^- \to ZH \to Z\gamma\gamma$, with the measurement of the partial $\gamma\gamma$ width, accessible through $\gamma\gamma$ production at a Compton collider: $\Gamma_{\rm tot} = \Gamma_i / BR_i$. In the upper part of the intermediate mass range, the combination of the branching ratios for $H \to WW$ and ZZ decays with the production cross sections for WW fusion and Higgs-strahlung [which can be expressed both by the partial Higgs-decay widths to WW and ZZ pairs], will allow us to extract the width of the Higgs particle. Thus, the width of the Higgs particle can be determined throughout the entire mass range.

2.4.3. Spin-parity

The angular distribution of the Z/H bosons in the Higgs-strahlung process is sensitive to the spin and parity of the Higgs particle [10]. Since the production amplitude is given by $\mathcal{A}(0^+) \sim \vec{\varepsilon}_{Z^*} \cdot \vec{\varepsilon}_Z$ the Z boson is produced in a state of longitudinal polarization at high energies – in accord with the equivalence theorem. As a result, the angular distribution

$$\frac{d\sigma}{d\cos\theta} \sim \sin^2\theta + \frac{8M_Z^2}{\lambda s} \tag{22}$$

approaches the spin-zero $\sin^2\theta$ law asymptotically. This may be contrasted with the distribution $\sim 1+\cos^2\theta$ for negative parity states which follows from the transverse polarization amplitude $\mathcal{A}(0^-) \sim \vec{\varepsilon}_{Z^*} \times \vec{\varepsilon}_Z \cdot \vec{k}_Z$. It is also characteristically different from the distribution of the background process $e^+e^- \to ZZ$ which, as a result of t/u-channel electron exchange, is strongly peaked in the forward/backward direction, Fig. 5.

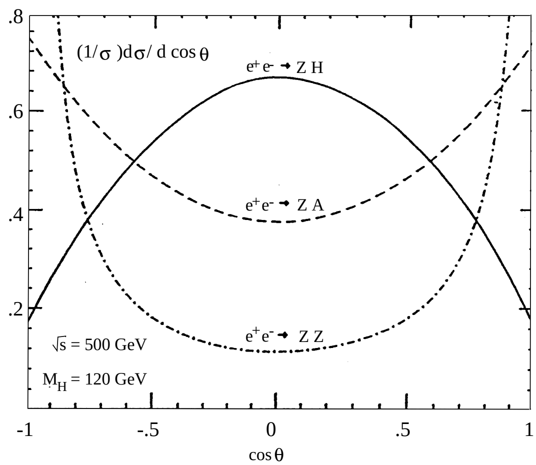

Fig. 5. Angular distribution of Z/H bosons in Higgs-strahlung, compared with the production of pseudoscalar particles and the ZZ background final states; Ref. [35].

In a similar way, the zero spin of the Higgs particle can be determined from the isotropic distribution of the decay products. Moreover, the parity can be measured by observing the spin correlations of the decay products. According to the equivalence theorem, the azimuthal angles of the decay planes in $H \to ZZ \to (\mu^+\mu^-)(\mu^+\mu^-)$ are asymptotically uncorrelated, $d\Gamma^+/d\phi_* \to 0$, for a 0^+ particle; this is to be contrasted with $d\Gamma^-/d\phi_* \to 1 - \frac{1}{4}\cos 2\phi_*$ for the distribution of the azimuthal angle between the planes for the decay of a 0^- particle. The difference between the distributions follows from the different polarizations of the vector bosons. While they approach longitudinal polarization states for scalar Higgs decays, they are transversely polarized for pseudoscalar particle decays.

2.4.4. Higgs couplings

Since the fundamental particles acquire masses by the interaction with the Higgs field, the strength of the Higgs couplings to fermions and gauge bosons is set by the masses of these particles. It will therefore be a very important task to measure these couplings, which are uniquely predicted by the very nature of the Higgs mechanism.

The Higgs couplings to massive gauge bosons can be determined from the production cross sections in Higgs-strahlung and WW, ZZ fusion, with the accuracy expected at the per-cent level. For heavy enough Higgs bosons the decay width can be exploited to determine the coupling to electroweak gauge bosons. For Higgs couplings to fermions the branching ratios $H \to b\bar{b}, c\bar{c}, \tau^+\tau^-$ can be used in the lower part of the intermediate mass range; these observables allow the direct measurement of the Higgs Yukawa couplings at the per-cent level. This is exemplified for a Higgs mass of 140 GeV in Fig. 6, a particularly interesting prediction being the ratio of the branching ratios $bb/\tau\tau = 3M_b^2(M_H^2)/M_\tau^2 \sim 10$.

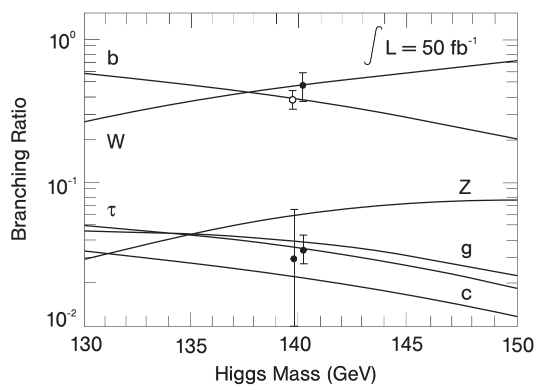

Fig. 6. The measurement of decay branching ratios of the SM Higgs boson for $M_H = 140$ GeV. In the bottom part of the figure the small error bar belongs to the τ branching ratio, the large bar to the average of the charm and gluon branching ratios which were not separated in the simulation of Ref. [36]. In the upper part of the figure the open circle denotes the b branching ratio, the full circle the W branching ratio.

A second interesting coupling is the Higgs coupling to top quarks. Since the top quark is by far the heaviest fermion in the Standard Model, irregularities in the standard picture of electroweak symmetry breaking through a fundamental Higgs field may become apparent in this coupling first. Thus the Htt Yukawa coupling may eventually provide essential clues to the nature of the mechanism breaking the electroweak symmetries.

Top loops mediating the production processes $gg \to H$ and $\gamma\gamma \to H$ (and the corresponding decay channels) give rise to cross sections and partial widths which are proportional to the square of the Higgs-top Yukawa coupling. The Yukawa coupling can be measured directly, for the lower part of the intermediate mass range, in the bremsstrahlung process $e^+e^- \to t\bar{t}H$ [37]. The Higgs boson is radiated predominantly from the heavy top quarks. Even though these experiments are difficult because of the small cross sections, *cf.* Fig. 7, and the complex topology of the $bbbbWW$ final state, this analysis is an important tool for exploring the mechanism of electroweak symmetry breaking. It has been shown in detailed experimental simulations [38] that the Htt Yukawa coupling can be measured in the bremsstrahlung process with an accuracy of about 10%. For large Higgs masses above the $t\bar{t}$ threshold, the decay channel $H \to t\bar{t}$ can be studied; in e^+e^- collisions the cross section of $e^+e^- \to t\bar{t}Z$ increases through the reaction $e^+e^- \to ZH(\to t\bar{t})$ [39].

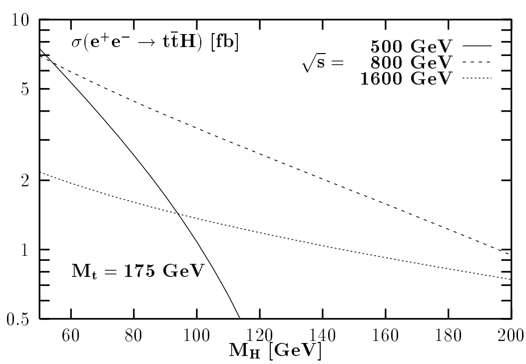

Fig. 7. The cross section for bremsstrahlung of SM Higgs bosons off top quarks in the Yukawa process $e^+e^- \to t\bar{t}H$. [The amplitude for radiation off the intermediate Z-boson line is small]; Ref. [37].

2.4.5. Higgs self-couplings

The Higgs mechanism, based on a non-zero value of the Higgs field in the vacuum, must finally be made manifest experimentally by reconstructing the interaction potential which generates the non-zero Higgs field in the vacuum. This program can be carried out by measuring the strength of the trilinear and quartic self-couplings of the Higgs particles:

$$g_{HHH} = 3(\sqrt{2}G_F)^{\frac{1}{2}} M_H^2 \,, \tag{23}$$

$$g_{HHHH} = 3(\sqrt{2}G_F) M_H^2 \,. \tag{24}$$

This is a very difficult task since the processes to be exploited are suppressed by small couplings and phase space. Nevertheless, the problem can be solved at e^+e^- linear colliders for sufficiently high luminosities [40]. The best suited reaction at e^+e^- colliders for the measurement of the trilinear coupling for Higgs masses in the theoretically preferred mass range of $\mathcal{O}(100\ \text{GeV})$, is double Higgs-strahlung:

$$e^+e^- \to ZHH \tag{25}$$

in which, among other mechanisms, the two-Higgs final state is generated by the exchange of a virtual Higgs particle so that this process is sensitive to the trilinear HHH coupling in the Higgs potential, Fig. 8. Since the cross section is only a fraction of 1 fb, an integrated luminosity of $\sim 1\,\text{ab}^{-1}$ is needed to isolate the events at linear colliders. The quartic coupling seems to be accessible only through loop effects in the foreseeable future.

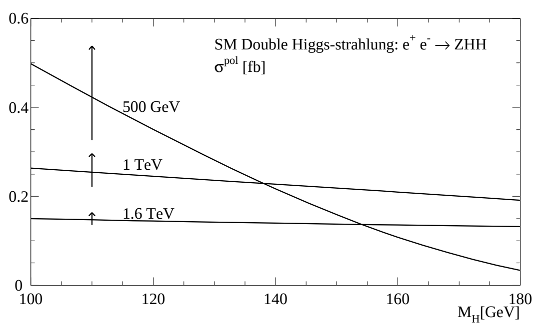

Fig. 8. The cross section for double Higgs-strahlung in e^+e^- collisions and the sensitivity to the trilinear Higgs coupling; Ref. [40].

To sum up, the essential elements of the Higgs mechanism can be established experimentally at the LHC and TeV e^+e^- linear colliders.

3. Higgs bosons in supersymmetric theories

Arguments rooted deeply in the Higgs sector, play an eminent role in introducing supersymmetry as a fundamental symmetry of Nature [11]. This is the only symmetry which correlates bosonic with fermionic degrees of freedom.

(a) The cancellation between bosonic and fermionic contributions to the radiative corrections of the light Higgs masses in supersymmetric theories provides a solution of the hierarchy problem in the Standard Model. If the Standard Model is embedded in a grand-unified theory, the large gap between the high grand-unification scale and the low scale of electroweak symmetry breaking can be stabilized in a natural way in boson-fermion symmetric theories [12, 41]. The radiative vector-boson correction is quadratically divergent, $\delta M_H^2(V) \sim \alpha[\Lambda^2 - M^2]$ so that for a cut-off scale $\Lambda \sim \Lambda_{\mathrm{GUT}}$ extreme fine-tuning between the intrinsic bare mass and the radiative quantum fluctuations would be needed to generate a Higgs mass of order M_W. However, as a consequence of Pauli's principle, the additional fermionic gaugino contributions in supersymmetric theories are just opposite in sign, $\delta M_H^2(\tilde{V}) \sim -\alpha[\Lambda^2 - \tilde{M}^2]$, so that the divergent terms cancel in the sum. Since $\delta M_H^2 \sim \alpha[\tilde{M}^2 - M^2]$, any fine-tuning is avoided for supersymmetric particle masses $\tilde{M} \lesssim \mathcal{O}(1\ \mathrm{TeV})$. Thus, within this symmetry scheme the Higgs sector is stable in the low-energy range $M_H \sim M_W$ even in the context of high-energy GUT scales.

(b) The concept of supersymmetry is strongly supported by the successful prediction of the electroweak mixing angle in the minimal version of this theory [13]. The extended particle spectrum of this theory drives the evolution of the electroweak mixing angle from the GUT value 3/8 down to $\sin^2\theta_W = 0.2336 \pm 0.0017$, the error including unknown threshold contributions at the low and the high supersymmetric mass scales. The prediction coincides with the experimentally measured value $\sin^2\theta_W^{\mathrm{exp}} = 0.2316 \pm 0.0002$ within the theoretical uncertainty of less than 2 per mille.

(c) Conceptually very interesting is the interpretation of the Higgs mechanism in supersymmetric theories as a quantum effect [42]. The breaking of the electroweak symmetry $\mathrm{SU(2)_L} \times \mathrm{U(1)}_Y$ can be induced radiatively while leaving the electromagnetic gauge symmetry $\mathrm{U(1)_{EM}}$ and the color gauge symmetry $\mathrm{SU(3)_C}$ unbroken for top-quark masses between 150 and 200 GeV. Starting with a set of universal scalar masses at the high GUT scale, the squared mass parameter of the Higgs sector evolves to negative values at the low electroweak scale while the squared squark and slepton masses remain positive.

The Higgs sector of supersymmetric theories differs in several aspects from the Standard Model [14]. To preserve supersymmetry and gauge invariance, at least two iso-doublet fields must be introduced, leaving us with a spectrum of five or more physical Higgs particles. In the minimal supersymmetric extension of the Standard Model (MSSM) the Higgs self-interactions are generated by the scalar-gauge superaction so that the quartic couplings are related to the gauge couplings in this scenario. This leads to strong bounds of less than about 130 GeV for the mass of the lightest Higgs boson [15]. If the system is assumed to remain weakly interacting up to scales of the order of the GUT or Planck scale, the mass remains small, for reasons quite analogous to the Standard Model, even in more complex supersymmetric theories involving additional Higgs fields and Yukawa interactions. The masses of the heavy Higgs bosons are expected to be of the scale of electroweak symmetry breaking up to order 1 TeV.

3.1. The Higgs sector of the MSSM

The particle spectrum of the MSSM [11] consists of leptons, quarks and their scalar supersymmetric partners, and of gauge particles, Higgs particles and their spin-1/2 superpartners.

Decomposing the superfields into fermionic and bosonic components, the following Lagrangeans can be derived, describing the interactions of the gauge, matter and Higgs fields:

$$\begin{aligned}
\mathcal{L}_V &= -\frac{1}{4}F_{\mu\nu}F_{\mu\nu} + \ldots + \frac{1}{2}D^2\,, \\
\mathcal{L}_\phi &= |D_\mu\phi|^2 + \ldots + \frac{g}{2}D|\phi|^2\,, \\
\mathcal{L}_W &= -\left|\frac{\partial W}{\partial\phi}\right|^2 .
\end{aligned}$$

The D field is an auxiliary field which does not propagate in space-time and which can be eliminated by applying the equations of motion: $D = -\frac{g}{2}|\phi|^2$. Reinserted into the Lagrangean, the quartic coupling of the scalar Higgs fields turns out to be

$$\mathcal{L}[\phi^4] = -\frac{g^2}{8}|\phi^2|^2. \tag{26}$$

Thus, the quartic coupling of the Higgs fields is given, in the minimal supersymmetric theory, by the square of the gauge coupling. Unlike the Standard Model, this coupling is not a free parameter. Moreover, the coupling is weak.

Two independent Higgs doublet fields H_1 and H_2 must be introduced into the superpotential,

$$W = -\mu\varepsilon_{ij}\hat{H}_1^i\hat{H}_2^j + \varepsilon_{ij}[f_1\hat{H}_1^i\hat{L}^j\hat{R} + f_2\hat{H}_1^i\hat{Q}^j\hat{D} + f_2'\hat{H}_2^j\hat{Q}^i\hat{U}]\,, \tag{27}$$

to provide masses to the down-type particles (H_1) and the up-type particles (H_2). Unlike the Standard Model, the second Higgs field cannot be identified with the charge conjugate of the first Higgs field since the superpotential must be analytic to preserve supersymmetry. Moreover, the Higgsino fields associated with a single Higgs field would generate triangle anomalies; they cancel if the two conjugate doublets are added up, and the classical gauge invariance of the interactions is not destroyed at the quantum level. Integrating the superpotential over the Grassmann coordinates generates the supersymmetric Higgs self-energy $V_0 = |\mu|^2(|H_1|^2 + |H_2|^2)$. The breaking of supersymmetry can be incorporated in the Higgs sector by introducing additional bilinear mass terms $\mu_{ij} H_i H_j$. Added to the supersymmetric self-energy part H^2 and the part H^4 generated by the gauge action, they lead to the following Higgs potential:

$$\begin{aligned} V &= m_1^2 H_1^{*i} H_1^i + m_2^2 H_2^{*i} H_2^i - m_{12}^2(\varepsilon_{ij} H_1^i H_2^j + \text{h.c.}) \\ &\quad + \frac{1}{8}(g^2 + g'^2)[H_1^{*i} H_1^i - H_2^{*i} H_2^i]^2 + \frac{1}{2} g^2 |H_1^{*i} H_2^{*i}|^2 . \end{aligned} \tag{28}$$

The Higgs potential includes three bilinear mass terms while the strength of the quartic couplings is set by the $\mathrm{SU}(2)_{\mathrm{L}}$ and $\mathrm{U}(1)_Y$ gauge couplings squared. The three mass terms are free parameters.

Expanding the fields about the ground state values v_1 and v_2, the mass eigenstates are given by the neutral states h^0, H^0 and A^0, which are even and odd under $\mathcal{CP}$ transformations, and by the two charged states $H^\pm$. After introducing the three parameters

$$\begin{aligned} M_Z^2 &= \frac{1}{2}(g^2 + g'^2)(v_1^2 + v_2^2)\,, \qquad \tan\beta = \frac{v_2}{v_1}\,, \\ M_A^2 &= m_{12}^2 \frac{v_1^2 + v_2^2}{v_1 v_2}\,, \end{aligned} \tag{29}$$

the mass matrix can be decomposed into three 2×2 blocks which are easy to diagonalize:

<u>charged</u> : $M_{H^\pm}^2 = M_A^2 + M_W^2$

<u>pseudoscalar</u> : M_A^2

<u>scalar</u> : $M_{h,H}^2 = \frac{1}{2}\left[M_A^2 + M_Z^2 \mp \sqrt{(M_A^2 + M_Z^2)^2 - 4 M_A^2 M_Z^2 \cos^2 2\beta}\right]$

$$\mathrm{tg}2\alpha = \mathrm{tg}2\beta \frac{M_A^2 + M_Z^2}{M_A^2 - M_Z^2} \quad \text{with} \quad -\frac{\pi}{2} < \alpha < 0\,.$$

From the mass formulae, two important inequalities can readily be derived,

$$M_h \leq M_Z,\ M_A \leq M_H\,, \tag{30}$$

$$M_W \leq M_{H^\pm} \tag{31}$$

which, by construction, are valid in the tree approximation. As a result, the lightest of the scalar Higgs masses is predicted to be bound by the Z mass, *modulo* radiative corrections. These bounds follow from the fact that the quartic coupling of the Higgs fields is determined in the MSSM by the size of the gauge couplings squared.

SUSY radiative corrections

The tree-level relations between the Higgs masses are strongly modified by radiative corrections involving the supersymmetric particle spectrum of the top sector [43]. These effects are proportional to the fourth power of the top mass. Their origin are incomplete cancellations between virtual top and stop loops, reflecting the breaking of supersymmetry. Moreover, the mass relations are affected by the potentially large mixing between $\tilde{t}_{\mathrm{L}}$ and $\tilde{t}_{\mathrm{R}}$ due to the top Yukawa coupling.

To leading order in M_t^4 these radiative corrections can be summarized in the parameter

$$\varepsilon = \frac{3G_{\mathrm{F}}}{\sqrt{2}\pi^2}\frac{M_t^4}{\sin^2\beta}\log\frac{M_s^2}{M_t^2}\,, \tag{32}$$

where the supersymmetry-breaking scale is identified with a common scalar quark mass M_s; if stop mixing effects are modest, they can be accounted for by shifting M_s^2 by the amount $\Delta M_s^2 = \hat{A}_t^2(1-\hat{A}_t^2/12M_s^2)$. In this approximation the light Higgs mass M_h can be expressed by M_A and tgβ in the following compact form:

$$M_h^2 = \frac{1}{2}\Big[M_A^2 + M_Z^2 + \varepsilon - \sqrt{(M_A^2+M_Z^2+\varepsilon)^2 - 4M_A^2M_Z^2\cos^2 2\beta - 4\varepsilon(M_A^2\sin^2\beta + M_Z^2\cos^2\beta)}\Big]. \tag{33}$$

The heavy Higgs masses M_H and $M_{H^\pm}$ follow from the sum rules

$$\begin{aligned} M_H^2 &= M_A^2 + M_Z^2 - M_h^2 + \varepsilon\,, \\ M_{H^\pm}^2 &= M_A^2 + M_W^2\,. \end{aligned} \tag{34}$$

Finally, the mixing parameter α which diagonalizes the $\mathcal{CP}$-even mass matrix, is given by the radiatively improved relation:

$$\mathrm{tg}2\alpha = \mathrm{tg}2\beta\frac{M_A^2+M_Z^2}{M_A^2-M_Z^2+\varepsilon/\cos 2\beta} \quad \text{with} \quad -\frac{\pi}{2} < \alpha < 0\,. \tag{35}$$

The spectrum of Higgs masses M_h, M_H and $M_{H^\pm}$ is displayed as a function of the pseudoscalar mass M_A in Fig. 9 for two representative values tg$\beta = 1.5$ and 30. For large A mass, the masses of the heavy Higgs particles coincide approximately, $M_A \simeq M_H \simeq M_{H^\pm}$, while the light Higgs mass approaches a small asymptotic value. The spectrum for large values of tgβ is highly regular: For small M_A, one finds $\{M_h \simeq M_A, M_H, M_{H^\pm} \simeq \text{const}\}$, for large M_A the opposite relationship $\{M_h \simeq \text{const}, M_H \simeq M_{H^\pm} \simeq M_A\}$.

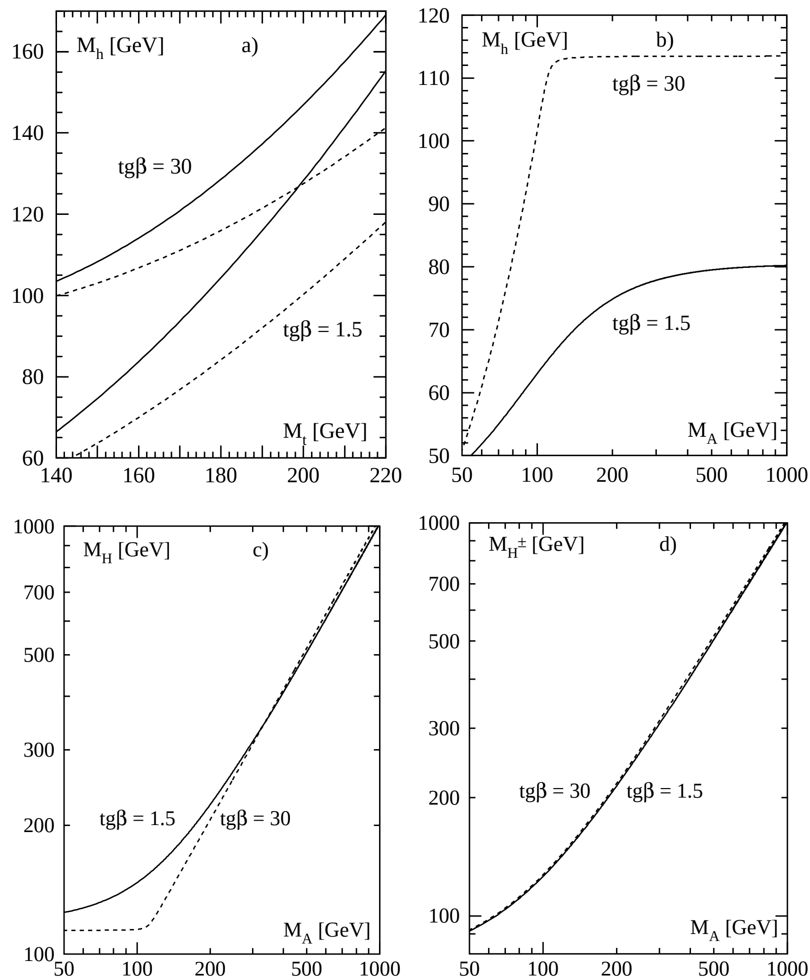

Fig. 9. (a) The upper limit on the light scalar Higgs pole mass in the MSSM as a function of the top quark mass for two values of tg$\beta = 1.5, 30$; the common squark mass has been chosen as $M_S = 1$ TeV. The full lines correspond to the maximal mixing case $[A_t = \sqrt{6}M_S,\ A_b = \mu = 0]$ and the dashed lines to vanishing mixing. The pole masses of the other Higgs bosons, $H, H^\pm$, are shown as a function of the pseudoscalar mass in (b)–(d) for two values of tg$\beta = 1.5, 30$, vanishing mixing and $M_t = 175$ GeV.

Upper bounds on the light Higgs mass are shown in Fig. 9(a) for two representative values $\mathrm{tg}\beta = 1.5$ and 30. The curves either do not include or do include mixing effects. It turns out that M_h is limited to about $M_h \lesssim 100$ GeV for moderate values of $\mathrm{tg}\beta$ while the general upper bound is given by $M_h \lesssim 130$ GeV, including large values of $\mathrm{tg}\beta$. The light Higgs sector can therefore be covered for small $\mathrm{tg}\beta$ entirely by the LEP2 experiments.

The two ranges of $\mathrm{tg}\beta$ near $\mathrm{tg}\beta \sim 1.7$ and $\mathrm{tg}\beta \sim M_t/M_b \sim 30$ to 50 are theoretically preferred in the MSSM if the model is embedded in a grand-unified scenario [44]. Given the experimentally observed top quark mass, universal τ and b masses at the unification scale can be evolved down to the experimental mass values at low energies in these two ranges of $\mathrm{tg}\beta$. Tuning problems in adjusting the τ/b mass ratio affect the large $\mathrm{tg}\beta$ solution. Nevertheless, this solution is attractive as the SO(10) symmetry relation between $\tau/b/t$ masses can be accommodated in this scenario.

3.2. SUSY Higgs couplings to SM particles

The size of MSSM Higgs couplings to quarks, leptons and gauge bosons is similar to the Standard Model, yet modified by the mixing angles α and β. Normalized to the SM values, they are listed in Table II. The pseudoscalar Higgs boson A does not couple to gauge bosons at the tree level but the coupling, compatible with $\mathcal{CP}$ symmetry, can be generated by higher-order loops. The charged Higgs bosons couple to up and down fermions with the left- and right-chiral amplitudes $g_\pm = -\frac{1}{\sqrt{2}}\left[g_t(1 \mp \gamma_5) + g_b(1 \pm \gamma_5)\right]$, where $g_{t,b} = (\sqrt{2}G_\mathrm{F})^{\frac{1}{2}} m_{t,b}$.

TABLE II

Higgs couplings in the MSSM to fermions and gauge bosons [$V = W, Z$] relative to SM couplings.

Φ		g_u^Φ	g_d^Φ	g_V^Φ
SM	H	1	1	1
MSSM	h	$\cos\alpha/\sin\beta$	$-\sin\alpha/\cos\beta$	$\sin(\beta-\alpha)$
	H	$\sin\alpha/\sin\beta$	$\cos\alpha/\cos\beta$	$\cos(\beta-\alpha)$
	A	$1/\mathrm{tg}\beta$	$\mathrm{tg}\beta$	0

The modified couplings incorporate the renormalization due to SUSY radiative corrections to leading order in M_t if the mixing angle α is related to β and M_A through the corrected formula Eq. (35). The behavior of the couplings as a function of mass M_A is exemplified in Fig. 10. For large M_A, in practice $M_A \gtrsim 200$ GeV, the couplings of the light Higgs boson h to the fermions and gauge bosons approach asymptotically the SM values. This is the essence of the decoupling theorem: Particles with large masses must decouple from the light particle system as a consequence of the quantum-mechanical uncertainty principle.

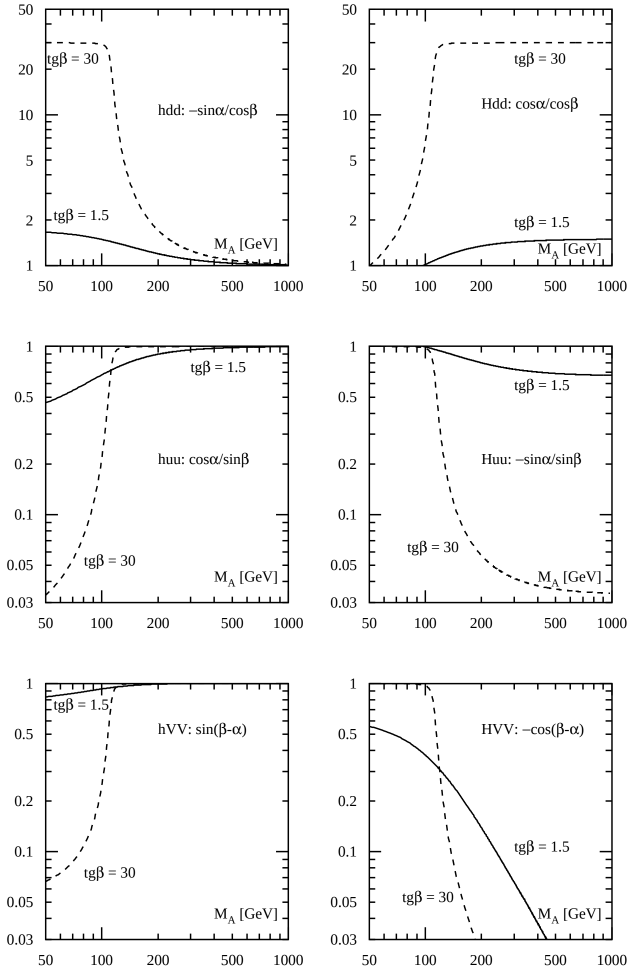

Fig. 10. The coupling parameters of the neutral MSSM Higgs bosons as a function of the pseudoscalar mass M_A for two values of tg$\beta = 1.5$, 30 and vanishing mixing. The couplings are defined in Table II.

3.3. Decays of Higgs particles

The light neutral Higgs boson h will decay mainly into fermion pairs since its mass is smaller than ~ 130 GeV, Fig. 11(a) (*cf.* Ref. [45] for a comprehensive summary). This is in general also the dominant decay mode of the pseudoscalar boson A. For values of tgβ larger than one and for masses less than ~ 140 GeV, the main decay modes of the neutral Higgs bosons are decays into bb and $\tau\tau$ pairs; the branching ratios are of order $\sim 90\%$ and 8%, respectively. The decays into cc pairs and gluons are suppressed especially for large tgβ. For large masses, the top decay channels $H, A \to t\bar{t}$ open up; yet for large tgβ this mode remains suppressed and the neutral Higgs bosons decay almost exclusively into bb and $\tau\tau$ pairs. If the mass is large enough, the heavy $\mathcal{CP}$-even Higgs boson H can in principle decay into weak gauge bosons, $H \to WW, ZZ$. Since the partial widths are proportional to $\cos^2(\beta - \alpha)$, they are strongly suppressed in general, and the gold-plated ZZ signal of the heavy Higgs boson in the Standard Model is lost in the supersymmetric extension. As a result, the total widths of the Higgs bosons rise

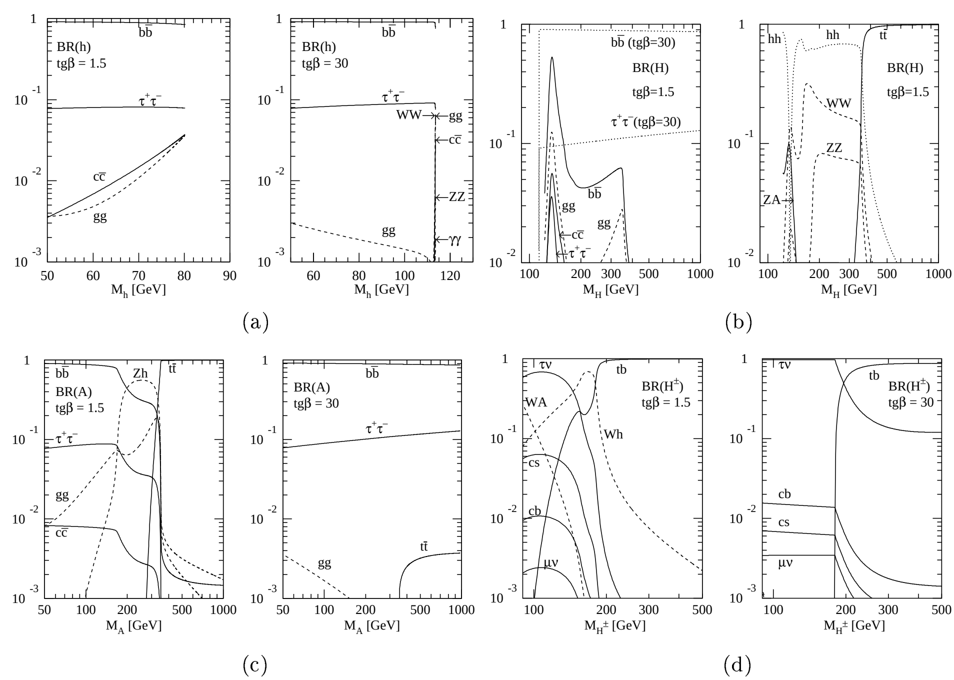

Fig. 11. Branching ratios of the MSSM Higgs bosons h — (a), H — (b), A — (c), $H^{\pm}$ — (d) for non-SUSY decay modes as a function of their masses for two values of tg$\beta = 1.5, 30$ and vanishing mixing. The common squark mass has been chosen as $M_S = 1$ TeV.

only linearly with the masses and they are much smaller in supersymmetric theories than in the Standard Model.

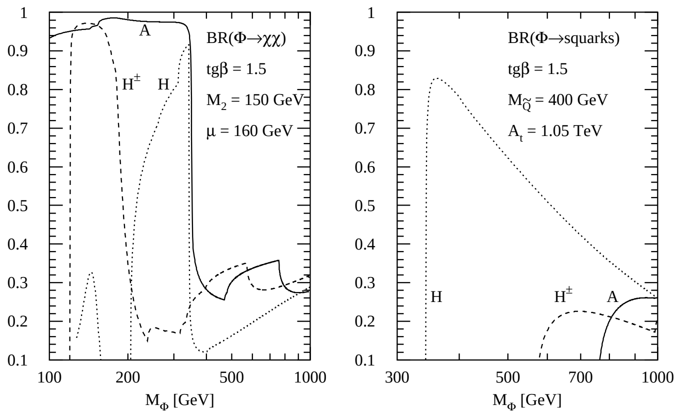

Fig. 12. Branching ratios of the MSSM Higgs boson $H, A, H^{\pm}$ decays into charginos/neutralinos and squarks as a function of their masses for tgβ = 1.5. The mixing parameters have been chosen as $\mu = 160$ GeV, $A_t = 1.05$ TeV, $A_b = 0$ and the squark masses of the first two generations as $M_{\tilde{Q}} = 400$ GeV. The gaugino mass parameter has been set to $M_2 = 150$ GeV.

The heavy neutral Higgs boson H can also decay into two lighter Higgs bosons. Other possible channels are Higgs cascade decays and decays into supersymmetric particles [46, 48], Fig. 12. In addition to light sfermions, Higgs boson decays into charginos and neutralinos could eventually be important. These new channels are kinematically accessible at least for the heavy Higgs bosons H, A and $H^{\pm}$; in fact, the branching fractions can be very large and they can become even dominant in some regions of the MSSM parameter space. Decays of h into the lightest neutralinos (LSP) are also important, exceeding 50% in some parts of the parameter space. These decays strongly affect experimental search techniques.

The *charged Higgs particles $H^{\pm}$* decay into fermions but also, if allowed kinematically, into the light neutral Higgs and a W boson. Below the tb and Wh thresholds, the charged Higgs particles will decay mostly into $\tau\nu_\tau$ and cs pairs, the former being dominant for tg$\beta > 1$. For large $M_{H^{\pm}}$ values, the top-bottom decay mode $H^+ \to t\bar{b}$ becomes dominant. In some parts of the SUSY parameter space, decays into supersymmetric particles may exceed 50 per cent.

Adding up the various decay modes, the width of all five Higgs bosons remains very narrow, being of order 10 GeV even for large masses.

3.4. The production of SUSY Higgs particles in e^+e^- collisions

The search for the neutral SUSY Higgs bosons at e^+e^- linear colliders will be a straightforward extension of the experiments presently performed at LEP2, which are expected to cover the mass range up to $\gtrsim$ 100 GeV for neutral Higgs bosons, depending on tgβ. Higher energies, $\sqrt{s}$ in excess of 250 GeV, are required to sweep the entire parameter space of the MSSM.

The main production mechanisms of <u>*neutral Higgs bosons*</u> at e^+e^- colliders [15, 47, 49] are the Higgs-strahlung process and associated pair production, as well as the fusion process:

$$\begin{array}{llcll} \text{(a)} & \text{Higgs} - \text{strahlung}: & e^+e^- & \xrightarrow{Z} & Z + h/H\,, \\ \text{(b)} & \text{pair production} \quad : & e^+e^- & \xrightarrow{Z} & A + h/H\,, \\ \text{(c)} & \text{fusion process} \quad\;\; : & e^+e^- & \xrightarrow{WW} & \overline{\nu_e}\,\nu_e\ + h/H\,. \end{array}$$

The $\mathcal{CP}$–odd Higgs boson A cannot be produced in fusion processes to leading order. The cross sections for the four Higgs-strahlung and pair production processes can be written as

$$\begin{aligned} \sigma(e^+e^- \to Z + h/H) &= \sin^2/\cos^2(\beta-\alpha)\ \sigma_{\rm SM}, \\ \sigma(e^+e^- \to A + h/H) &= \cos^2/\sin^2(\beta-\alpha)\ \bar{\lambda}\ \sigma_{\rm SM}, \end{aligned} \tag{36}$$

where $\sigma_{\rm SM}$ is the SM cross section for Higgs-strahlung and the coefficient $\bar{\lambda} \sim \lambda_{Aj}^{3/2}/\lambda_{Zj}^{1/2}$ accounts for the suppression of the P–wave Ah/H cross sections near the threshold.

The cross sections for Higgs-strahlung and for pair production, likewise the cross sections for the production of the light and the heavy neutral Higgs bosons h and H, are mutually complementary to each other, coming either with coefficients $\sin^2(\beta-\alpha)$ or $\cos^2(\beta-\alpha)$. As a result, since $\sigma_{\rm SM}$ is large, at least the lightest $\mathcal{CP}$-even Higgs boson must be detected.

Representative examples of the cross sections for the production mechanisms of the neutral Higgs bosons are shown as a function of the Higgs masses in Fig. 13 for tg$\beta = 1.5$ and 30. The cross section for hZ is large for M_h near the maximum value allowed for tgβ; it is of order 50 fb, corresponding to $\sim$ 50,000 events for an integrated luminosity of 1 ab^{-1}. By contrast, the cross section for HZ is large if M_h is sufficiently below the maximum value [implying small M_H]. For h and for light H, the signals consist of a Z boson accompanied by a bb or $\tau\tau$ pair. These signals are easy to separate from the background which comes mainly from ZZ production if the Higgs mass is close to M_Z. For the associated channels $e^+e^- \to Ah$ and AH, the situation is opposite to the previous case: The cross section for Ah is large for light h whereas AH pair production is the dominant mechanism in the complementary region for heavy H and A bosons. The sum of the two cross

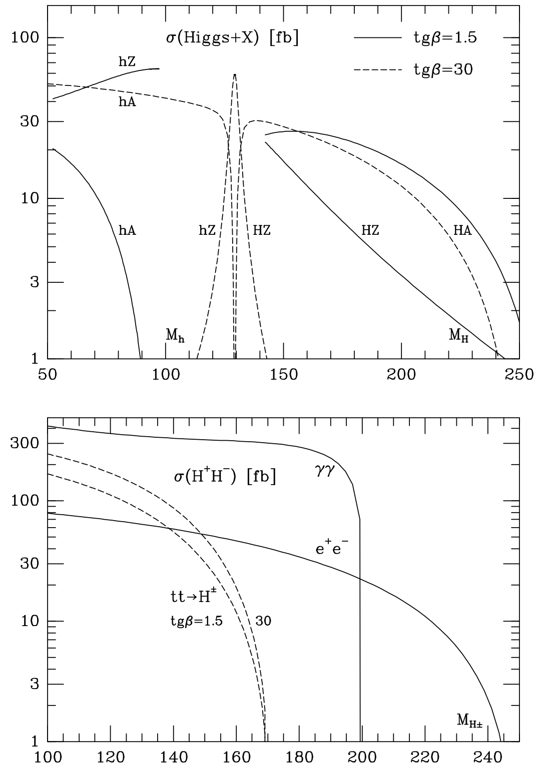

Fig. 13. Production cross sections of MSSM Higgs bosons at $\sqrt{s} = 500$ GeV: Higgs-strahlung and pair production; upper part: neutral Higgs bosons, lower part: charged Higgs bosons. Ref. [45].

sections decreases from ~ 50 to 10 fb if M_A increases from ~ 50 to 200 GeV at $\sqrt{s} = 500$ GeV. In major parts of the parameter space, the signals consist of four b quarks in the final state, requiring efficient b quark tagging. Mass constraints will help to eliminate the backgrounds from QCD jets and ZZ final states. For the WW fusion mechanism, the cross sections are larger than for Higgs-strahlung if the Higgs mass is moderately small, *i.e.* less than 160 GeV at $\sqrt{s} = 500$ GeV. However, since the final state cannot be fully reconstructed, the signal is more difficult to extract. As in the case of Higgs-strahlung , the production of light h and heavy H Higgs bosons complement each other in WW fusion, too.

The *charged Higgs bosons*, if lighter than the top quark, can be produced in top decays, $t \to b + H^+$, with a branching ratio varying between 2% and 20% in the kinematically allowed region. Since the cross section for top-pair production is of order 0.5 pb at $\sqrt{s} = 500$ GeV, this corresponds to 20,000 to 200,000 charged Higgs bosons at a luminosity of 1 ab^{-1}. Since for tgβ larger than one, the charged Higgs bosons will decay mainly to $\tau\nu_\tau$, resulting in a surplus of τ final states over e, μ final states in t decays, an apparent breaking of lepton universality. For large Higgs masses the dominant decay mode is the top decay $H^+ \to t\bar{b}$. In this case the charged Higgs particles must be pair produced in e^+e^- colliders:

$$e^+e^- \to H^+H^- \, .$$

The cross section depends only on the charged Higgs mass. It is of order 100 fb for small Higgs masses at $\sqrt{s} = 500$ GeV, but it drops very quickly due to the P–wave suppression $\sim \beta^3$ near the threshold. For $M_{H^\pm} = 230$ GeV, the cross section falls to a level of $\simeq 5$ fb, which for an integrated luminosity of 1 ab^{-1} corresponds to 5,000 events. The cross section is considerably larger for $\gamma\gamma$ collisions.

Experimental Search Strategies

The search strategies have been summarized for neutral Higgs bosons in Refs [50, 51] and for charged Higgs bosons in Ref. [52]. Visible as well as invisible decays are under experimental control already for an integrated luminosity of 10 fb^{-1}. The experimental situation can be summarized in the following two points:

(i) The light $\mathcal{CP}$-even Higgs particle h can be detected in the entire range of the MSSM parameter space, either via the Higgs-strahlung process $e^+e^- \to hZ$ or via pair production $e^+e^- \to hA$. This conclusion holds true even at a c.m. energy of 250 GeV, independently of the squark mass values; it is also valid if decays to invisible neutralino and other SUSY particles are realized in the Higgs sector.

(ii) The area in the parameter space where *all SUSY Higgs bosons* can be discovered at e^+e^- colliders is characterized by $M_H, M_A \lesssim \frac{1}{2}\sqrt{s}$, independently of tg$\beta$. The h, H Higgs bosons can be produced either via Higgs-strahlung or in Ah, AH associated production; charged Higgs bosons will be produced in H^+H^- pairs.

3.5. Measuring the parity of the H, A bosons

Once the Higgs bosons are discovered, the properties of the particles must be established. Besides the reconstruction of the supersymmetric Higgs potential [53], a very demanding effort, the external quantum numbers must be established, in particular the parity of the heavy scalar and pseudoscalar Higgs particles H and A [55].

For large H, A masses the decays $H, A \to t\bar{t}$ to top final states can be used to discriminate between the different parity assignments [55]. For example, the W^+ and W^- bosons in the t and $\bar{t}$ decays tend to be emitted antiparallel and parallel in the plane perpendicular to the $t\bar{t}$ axis,

$$\frac{d\Gamma^{\pm}}{d\phi_*} \propto 1 \mp \left(\frac{\pi}{4}\right)^2 \cos\phi_* \,, \tag{37}$$

for H and A decays, respectively.

For light H, A masses, $\gamma\gamma$ collisions appear to provide a viable solution [55]. The fusion of Higgs particles in linearly polarized photon beams depends on the angle between the polarization vectors. For scalar 0^+ particles the production amplitude is non-zero for parallel polarization vectors while pseudoscalar 0^- particles require perpendicular polarization vectors:

$$\begin{aligned} \mathcal{M}(H)^+ &\sim \vec{\varepsilon}_1 \cdot \vec{\varepsilon}_2 \,, \\ \mathcal{M}(A)^- &\sim \vec{\varepsilon}_1 \times \vec{\varepsilon}_2 \,. \end{aligned} \tag{38}$$

The experimental set-up for Compton back-scattering of laser light can be tuned in such a way that the linear polarization of the hard-photon beams approaches values close to 100%. Depending on the parity $\pm$ of the resonance produced, the measured asymmetry for photons polarized parallel or perpendicular,

$$\mathcal{A} = \frac{\sigma_{\parallel} - \sigma_{\perp}}{\sigma_{\parallel} + \sigma_{\perp}} \tag{39}$$

is either positive or negative.

3.6. The SUSY Higgs potential

The minimal supersymmetric extension of the Standard Model (MSSM) includes two iso-doublets of Higgs fields φ_1, φ_2.

The general self-interaction potential of two Higgs doublets φ_i in a $\mathcal{CP}$-conserving theory can be expressed by seven real couplings λ_k and three real mass parameters m_{11}^2, m_{22}^2 and m_{12}^2:

$$\begin{aligned} V[\varphi_1, \varphi_2] &= m_{11}^2 \varphi_1^\dagger \varphi_1 + m_{22}^2 \varphi_2^\dagger \varphi_2 - [m_{12}^2 \varphi_1^\dagger \varphi_2 + \text{h.c.}] \\ &+ \tfrac{1}{2}\lambda_1 (\varphi_1^\dagger \varphi_1)^2 + \tfrac{1}{2}\lambda_2 (\varphi_2^\dagger \varphi_2)^2 + \lambda_3 (\varphi_1^\dagger \varphi_1)(\varphi_2^\dagger \varphi_2) + \lambda_4 (\varphi_1^\dagger \varphi_2)(\varphi_2^\dagger \varphi_1) \\ &+ \left\{ \tfrac{1}{2}\lambda_5 (\varphi_1^\dagger \varphi_2)^2 + [\lambda_6 (\varphi_1^\dagger \varphi_1) + \lambda_7 (\varphi_2^\dagger \varphi_2)] \varphi_1^\dagger \varphi_2 + \text{h.c.} \right\} \end{aligned}$$

In the MSSM, the λ parameters are given at the tree level by

$$\begin{aligned} &\lambda_1 = \lambda_2 = \tfrac{1}{4}(g^2 + g'^2) \,, \quad \lambda_3 = \tfrac{1}{4}(g^2 - g'^2) \,, \quad \lambda_4 = -\tfrac{1}{2} g^2 \,, \\ &\lambda_5 = \lambda_6 = \lambda_7 = 0 \end{aligned} \tag{40}$$

and the mass parameters by

$$\begin{aligned} m_{11}^2 &= (M_A^2 + M_Z^2)\sin^2\beta - \tfrac{1}{2}M_Z^2, \qquad m_{12}^2 = \tfrac{1}{2}M_A^2 \sin 2\beta, \\ m_{22}^2 &= (M_A^2 + M_Z^2)\cos^2\beta - \tfrac{1}{2}M_Z^2\,. \end{aligned} \tag{41}$$

Including the radiative corrections in the one-loop leading top/stop approximation, the set of trilinear couplings between the neutral physical Higgs bosons can be written [53] in units of $\lambda_0 = M_Z^2/v$ as

$$\begin{aligned} \lambda_{hhh} &= 3\cos 2\alpha \sin(\beta+\alpha) + 3\frac{\varepsilon}{M_Z^2}\frac{\cos\alpha}{\sin\beta}\cos^2\alpha\,, \\ \lambda_{Hhh} &= 2\sin 2\alpha \sin(\beta+\alpha) - \cos 2\alpha \cos(\beta+\alpha) + 3\frac{\varepsilon}{M_Z^2}\frac{\sin\alpha}{\sin\beta}\cos^2\alpha \end{aligned} \tag{42}$$

etc. As expected, the self-coupling of the light $\mathcal{CP}$-even neutral Higgs boson h approaches the SM value $3M_H^2/M_Z^2$ in the decoupling limit.

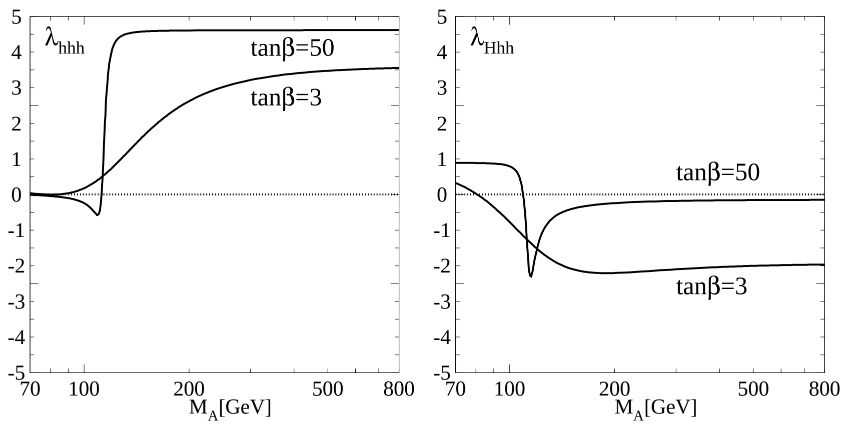

Fig. 14. Variation of the trilinear couplings between $\mathcal{CP}$-even Higgs bosons with M_A for tan$\beta = 3$ and 50 in the MSSM; the region of rapid variations corresponds to the h/H cross-over region in the neutral $\mathcal{CP}$-even sector.

The variation of the trilinear couplings with M_A is shown for two values $\tan\beta = 3$ and 50 in Fig. 14. The region in which the couplings vary rapidly, corresponds to the h/H cross-over region of the two mass branches in the neutral $\mathcal{CP}$-even sector, *cf.* Eq. (33).

In contrast to the Standard Model, resonance production of the heavy neutral Higgs boson H followed by subsequent decays $H \to hh$, plays a dominant role in part of the parameter space for moderate values of $\tan\beta$

and H masses between 200 and 350 GeV, Ref. [45]. In this range, the branching ratio, derived from the partial width

$$\Gamma(H \to hh) = \frac{\sqrt{2} G_{\mathrm{F}} M_Z^4 \beta_h}{32\pi M_H} \lambda_{Hhh}^2 \tag{43}$$

is neither too small nor too close to unity to be measured directly. [The decay of either h or H into a pair of pseudoscalar states, $h/H \to AA$, is kinematically not possible in the parameter range which the present analysis is based upon.] If double Higgs production is mediated by the resonant production of H, the total production cross section of light Higgs pairs increases by about an order of magnitude [53].

The trilinear Higgs-boson couplings are involved in a large set of processes at e^+e^- linear colliders [53, 40, 54]:

$$\begin{array}{llll} \text{double Higgs-strahlung:} & e^+e^- \to ZH_iH_j & \text{and} \quad ZAA & [H_{i,j} = h, H] \\ \text{ass. Higgs production} : & e^+e^- \to AH_iH_j & \text{and} \quad AAA & \\ WW \text{ fusion} : & e^+e^- \to \bar{\nu}_e \nu_e H_iH_j & \text{and} \quad \bar{\nu}_e \nu_e AA & \end{array}$$

TABLE III

The trilinear couplings between neutral $\mathcal{CP}$-even and $\mathcal{CP}$-odd MSSM Higgs bosons which can generically be probed in double Higgs-strahlung and associated triple Higgs-production, are marked by a cross. The matrix for WW fusion is isomorphic to the matrix for Higgs-strahlung.

	double Higgs-strahlung				triple Higgs-production			
λ	Zhh	ZHh	ZHH	ZAA	Ahh	AHh	AHH	AAA
hhh	×				×			
Hhh	×	×			×	×		
HHh		×	×			×	×	
HHH			×				×	
hAA				×	×	×		×
HAA				×		×	×	×

The trilinear couplings which enter for various final states, are marked by a cross in the matrix Table III. While the combination of couplings in Higgs-strahlung is isomorphic to WW fusion, it is different for associated triple Higgs production. If all the cross sections were large enough, the system could be solved for the whole set of λ's, up to discrete ambiguities, based on double Higgs-strahlung, Ahh and triple A production ["bottom-up approach"]. This can easily be inferred from the correlation matrix Table III.

From $\sigma(ZAA)$ and $\sigma(AAA)$ the couplings $\lambda(hAA)$ and $\lambda(HAA)$ can be extracted. In a second step, $\sigma(Zhh)$ and $\sigma(Ahh)$ can be used to solve for $\lambda(hhh)$ and $\lambda(Hhh)$; subsequently, $\sigma(ZHh)$ for $\lambda(HHh)$; and, finally, $\sigma(ZHH)$ for $\lambda(HHH)$. The remaining triple Higgs cross sections $\sigma(AHh)$ and $\sigma(AHH)$ provide additional redundant information on the trilinear couplings.

In practice, not all the cross sections will be large enough to be accessible experimentally, preventing the straightforward solution for the complete set of couplings. In this situation however the reverse direction can be followed ["top-down approach"]. The trilinear Higgs couplings can stringently be tested by comparing the theoretical predictions of the cross sections with the experimental results for the accessible channels of double and associated triple Higgs production.

The unpolarized cross section for double Higgs-strahlung, $e^+e^- \to Zhh$, is modified [53, 40] with regard to the Standard Model by H,A exchange diagrams:

$$\frac{d\sigma(e^+e^- \to Zhh)}{dx_1 dx_2} = \frac{\sqrt{2}G_F^3 M_Z^6}{384\pi^3 s} \frac{v_e^2 + a_e^2}{(1-\mu_Z)^2} \mathcal{Z}_{11} \tag{44}$$

with

$$\begin{aligned} \mathcal{Z}_{11} &= \mathfrak{z}^2 f_0 + \frac{\mathfrak{z}}{2}\left[\frac{\sin^2(\beta-\alpha) f_3}{y_1+\mu_{1Z}} + \frac{\cos^2(\beta-\alpha) f_3}{y_1+\mu_{1A}}\right] \\ &+ \frac{\sin^4(\beta-\alpha)}{4\mu_Z(y_1+\mu_{1Z})}\left[\frac{f_1}{y_1+\mu_{1Z}} + \frac{f_2}{y_2+\mu_{1Z}}\right] \\ &+ \frac{\cos^4(\beta-\alpha)}{4\mu_Z(y_1+\mu_{1A})}\left[\frac{f_1}{y_1+\mu_{1A}} + \frac{f_2}{y_2+\mu_{1A}}\right] \\ &+ \frac{\sin^2 2(\beta-\alpha)}{8\mu_Z(y_1+\mu_{1A})}\left[\frac{f_1}{y_1+\mu_{1Z}} + \frac{f_2}{y_2+\mu_{1Z}}\right] + \left\{ y_1 \leftrightarrow y_2 \right\} \end{aligned} \tag{45}$$

and

$$\begin{aligned} \mathfrak{z} &= \left[\frac{\lambda_{hhh}\sin(\beta-\alpha)}{y_3-\mu_{1Z}} + \frac{\lambda_{Hhh}\cos(\beta-\alpha)}{y_3-\mu_{2Z}}\right] \\ &\quad + \frac{2\sin^2(\beta-\alpha)}{y_1+\mu_{1Z}} + \frac{2\sin^2(\beta-\alpha)}{y_2+\mu_{1Z}} + \frac{1}{\mu_Z} \end{aligned} \tag{46}$$

with $\mu_1 = M_h^2/s$ and $\mu_2 = M_H^2/s$. The coefficients f_i are independent of the Higgs self-couplings; they are determined by the Higgs-gauge field couplings.

The total cross sections are shown in Fig. 15 for the e^+e^- collider energy $\sqrt{s} = 500$ GeV. The parameter $\tan\beta$ is chosen to be 3 and 50 and the mixing parameters $A = 1$ TeV and $\mu = -1$ TeV and 1 TeV, respectively. If $\tan\beta$ and the mass M_h are fixed, the masses of the other heavy Higgs bosons are predicted in the MSSM. Since the vertices are suppressed by sin / cos functions of the mixing angles β and α, the continuum hh cross sections are suppressed compared to the Standard Model. However, the size of the cross sections increases for moderate $\tan\beta$ by nearly an order of magnitude if the hh final state can be generated in the chain $e^+e^- \to ZH \to Zhh$ via resonant H Higgs-strahlung. If the light Higgs mass approaches the upper limit for a given value of $\tan\beta$, the decoupling theorem drives the cross section of the supersymmetric Higgs boson h back to its Standard Model value since the Higgs particles A, H, $H^\pm$ become asymptotically heavy in this limit. As a result of the decoupling theorem, resonance production is not effective for large tanβ. If the H mass is large enough to allow decays to hh pairs, the ZZH coupling is already too small to generate a sizable cross section.

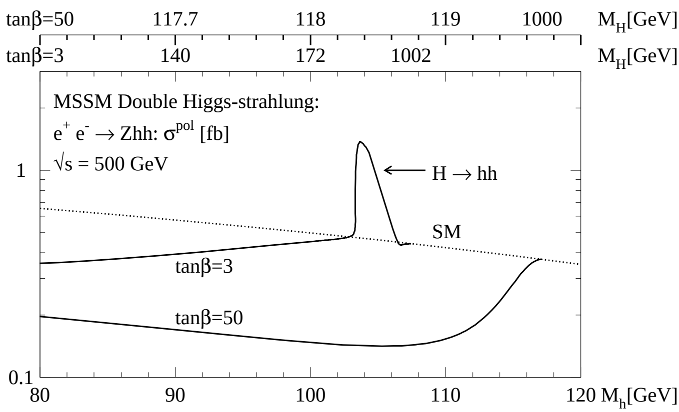

Fig. 15. Total cross sections for MSSM hh production via double Higgs-strahlung at e^+e^- linear colliders for $\tan\beta = 3$, 50 and $\sqrt{s} = 500$ GeV, including mixing effects ($A = 1$ TeV, $\mu = -1/1$ TeV for $\tan\beta = 3/50$). The dotted line indicates the SM cross section.

The 2-particle processes $e^+e^- \to ZH_i$ and $e^+e^- \to AH_i$ are among themselves and mutually complementary to each other in the MSSM [49], coming with the coefficients $\sin^2(\beta-\alpha)/\cos^2(\beta-\alpha)$ and $\cos^2(\beta-\alpha)/\sin^2(\beta-\alpha)$ for $H_i = h$, H, respectively. Since multi-Higgs final states are mediated by virtual h, H bosons, the two types of self-complementarity and mutual complementarity are also operative in double-Higgs production: $e^+e^- \to ZH_iH_j$, ZAA and AH_iH_j, AAA. As the different mechanisms are intertwined, the complementarity between these 3-particle final states is of more complex matrix form.

The results can be summarized in compact form by constructing sensitivity areas for the trilinear SUSY Higgs couplings based on the cross sections for double Higgs-strahlung and triple Higgs production. WW double-Higgs fusion can provide additional information on the Higgs self-couplings. The sensitivity areas will be defined in the $[M_A,\ \tan\beta]$ plane [40]. The criteria for accepting a point in the plane as accessible for the measurement of a specific trilinear coupling are set as follows:

$$\begin{aligned} &(i) && \sigma[\lambda] > 0.01 \text{ fb} \\ &(ii) && \text{var}\{\lambda \to (1 \pm \tfrac{1}{2})\lambda\} > 2 \text{ st.dev.}\{\lambda\} \quad \text{for} \quad \int \mathcal{L} = 2 \text{ ab}^{-1}\,. \end{aligned} \tag{47}$$

The first criterion demands at least 20 events in a sample collected for an integrated luminosity of 2 ab^{-1}, corresponding to about the lifetime of a high-luminosity machine such as TESLA. The second criterion demands a 50% change of the signal parameter to exceed a statistical fluctuation of 2 standard deviations. Even though the two criteria may look quite loose, tightening (i) and/or (ii) does not have a large impact on the size of the sensitivity areas in the $[M_A,\ \tan\beta]$ plane, see Ref. [54]. For the sake of simplicity, the e^+e^- beams are assumed to be unpolarized and mixing effects are neglected. Sensitivity areas of the trilinear couplings for processes defined in the correlation matrix Table III, are depicted in Fig. 16. If at most one heavy Higgs boson is present in the final states, the lower energy $\sqrt{s} = 500$ GeV is most preferable in the case of double Higgs-strahlung. HH final states in double Higgs-strahlung and triple Higgs production involving A give rise to larger sensitivity areas at the high energy $\sqrt{s} = 1$ TeV. Apart from small regions in which interference effects play a role, the magnitude of the sensitivity regions in the parameter $\tan\beta$ is readily explained by the

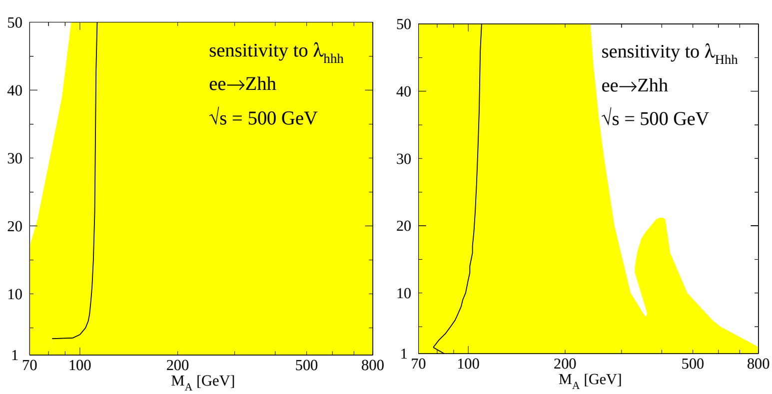

Fig. 16. Sensitivity to λ_{hhh} and λ_{Hhh} in the processes $e^+e^- \to Zhh$ for collider energy 500 GeV (no mixing). [Vanishing trilinear couplings are indicated by contour lines.]

magnitude of the parameters $\lambda\sin(\beta-\alpha)$ and $\lambda\cos(\beta-\alpha)$. For large M_A the sensitivity criteria cannot be met any more either as a result of phase space effects or due to the suppression of the H, A, $H^\pm$ propagators for large masses. While the trilinear coupling of the light neutral $\mathcal{CP}$-even Higgs boson is accessible in nearly the entire MSSM parameter space, the regions for λ's involving heavy Higgs bosons are rather restricted.

Since neither experimental efficiencies nor background related cuts are considered, the areas must be interpreted as maximal envelopes. They are expected to shrink when experimental efficiencies are properly taken into account; more elaborate cuts on signal and backgrounds, however, may help reduce their impact.

3.7. Non-minimal supersymmetric extensions

The minimal supersymmetric extension of the Standard Model (MSSM) may appear very restrictive for supersymmetric theories in general, in particular in the Higgs sector where the quartic couplings are identified with the gauge couplings. However, it turns out that the mass pattern of the MSSM is quite typical if the theory is assumed to be valid up to the GUT scale — the motivation for supersymmetry *per se*. This general pattern has been studied thoroughly within the next-to-minimal extension: The MSSM, incorporating two Higgs isodoublets, is augmented by introducing an isosinglet field N. This extension leads to a model [56, 57] which is generally referred to as the (M+1)SSM.

The additional Higgs singlet can solve the so-called μ–problem [*i.e.* $\mu\sim$ order M_W] by eliminating the higgsino parameter from the potential and by replacing this parameter by the vacuum expectation value of the N field, which can be naturally related to the usual vacuum expectation values of the Higgs isodoublet fields. In this scenario the superpotential involves the two trilinear couplings H_1H_2N and N^3. The consequences of this extended Higgs sector will be outlined in the context of (s)grand unification including universal soft breaking terms of the supersymmetry [57].

The Higgs spectrum of the (M+1)SSM includes, besides the minimal set of Higgs particles, one additional scalar and pseudoscalar Higgs particle. The neutral Higgs particles are in general mixtures of the iso-scalar doublets, which couple to W,Z bosons and fermions, and the iso-scalar singlet, decoupled from the non-Higgs sector. The trilinear self-interactions contribute to the masses of the Higgs particles. For the lightest Higgs boson of each species:

$$\begin{aligned} M^2(h_1) &\leq M_Z^2\cos^2 2\beta+\lambda^2v^2\sin^2 2\beta\,,\\ M^2(A_1) &\leq M_2(A)\,,\\ M^2(H^\pm) &\leq M^2(W)+M^2(A)-\lambda^2v^2\,, \end{aligned} \qquad (48)$$

where $M(A)$ is the pseudoscalar mass parameter of the MSSM subsystem. In contrast to the minimal model, the mass of the charged Higgs particle could be smaller than the W mass. Since the trilinear couplings increase with energy, upper bounds on the mass of the lightest neutral Higgs boson h_1 can be derived, in analogy to the Standard Model, from the assumption that the theory be valid up to the GUT scale: $m(h_1) \lesssim 140$ GeV. Thus despite the additional interactions, the distinct pattern of the minimal extension remains valid also in more complex supersymmetric scenarios [58]. In fact, the mass bound of 140 GeV for the lightest Higgs particle is realized in almost all supersymmetric theories. If h_1 is (nearly) purely iso-scalar, it decouples from the gauge-boson and fermion system and its role is taken by the next Higgs particle with a large isodoublet component, implying the validity of the mass bound again.

The couplings R_i of the $\mathcal{CP}$–even neutral Higgs particles h_i to the Z boson, ZZh_i, are defined relative to the usual SM coupling. If the Higgs particle h_1 is primarily isosinglet, the coupling R_1 is small and the particle cannot be produced by Higgs-strahlung. However, in this case h_2 is generally light and couples with sufficient strength to the Z boson; if not, h_3 plays this role. This scenario is quantified in Fig. 17 where the couplings R_1 and R_2 are shown for the ensemble of allowed Higgs masses $m(h_1)$ and $m(h_2)$

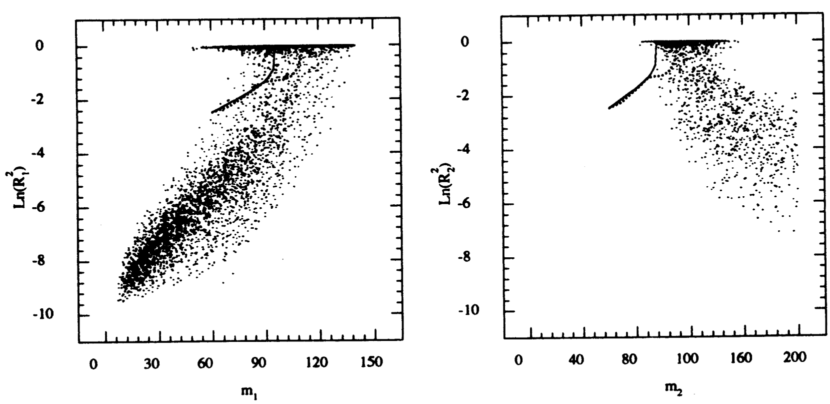

Fig. 17. The couplings ZZh_1 and ZZh_2 of the two lightest $\mathcal{CP}$–even Higgs bosons in the next-to-minimal supersymmetric extension of the Standard Model, (M + 1)SSM. The solid lines indicate the accessible range at LEP2, the dotted lines for an energy of 205 GeV. The scatter plots are solutions for an ensemble of possible SUSY parameters defined at the scale of grand unification. Ref. [57].

[adopted from Ref. [59]; see also Ref. [57, 60]]. Two different regions exist within the GUT (M+1)SSM: A densely populated region with $R_1 \sim 1$ and $m_1 > 50$ GeV, and a tail with $R_1 < 1$ to $\ll 1$ and small m_1. Within this tail, the lightest Higgs boson is essentially a gauge-singlet state so that it can escape detection at LEP [full/solid lines]. If the lightest Higgs boson is essentially a gauge singlet, the second lightest Higgs particle cannot be heavy. In the tail of diagram 17(a) the mass of the second Higgs boson h_2 varies between 80 GeV and, essentially, the general upper limit of $\sim$ 140 GeV. h_2 couples with full strength to Z bosons, $R_2 \sim 1$. If in the tail of diagram 17(b) this coupling becomes weak, the third Higgs boson will finally take the role of the leading light particle.

Summa. Experiments at e^+e^- colliders are in a no-lose situation [60] for detecting the Higgs particles in general supersymmetric theories, even for c.m. energies as low as $\sqrt{s} \sim 300$ GeV.

4. Strongly interacting *W* bosons

The Higgs mechanism is based on the theoretical concept of spontaneous symmetry breaking [1]. In the canonical formulation, which is adopted in the Standard Model, a four-component *fundamental* scalar field is introduced, which is endowed with a self-interation such that the field acquires a non-zero value in the ground state. The specific direction in isospace which is singled out by the ground-state solution, breaks the isospin invariance of the interaction spontaneously. The interaction of the gauge fields with the scalar field in the ground state generates the masses of these fields. The longitudinal degrees of freedom of the gauge fields are built up by absorption of the Goldstone modes which are associated with the spontaneous breaking of the electroweak symmetries in the scalar field sector. Fermions acquire masses through Yukawa interactions with the ground-state field. While three scalar components are absorbed by the gauge fields, one degree of freedom manifests itself as a physical particle, the Higgs boson. The exchange of this particle in scattering amplitudes including longitudinal gauge fields and massive fermion fields, ensures the unitarity of the theory up to asymptotic energies.

In the alternative to this scenario the spontaneous symmetry breaking is generated *dynamically* [2]. A system of new fermions is introduced which interact strongly at a scale of order 1 TeV. In the ground state of such a system a scalar condensate of fermion-antifermion pairs may form. Such a process is quite generally expected in any non-abelian gauge theory of the new strong interactions. Since the scalar condensate breaks the chiral symmetry of the fermion system, Goldstone fields will form which can be absorbed by the electroweak gauge fields to build up the longitudinal components and the masses of the gauge fields. Novel gauge interactions must be introduced which couple the leptons and quarks of the Standard Model to the new fermions in order to generate lepton and quark masses through interactions with the ground-state fermion-antifermion condensate. In the low-energy sector of the electroweak theory the fundamental Higgs-field approach and the dynamical alternative are equivalent. However the two theories are fundamentally different at high energies. While the unitarity of the electroweak gauge theory is guaranteed by the exchange of the scalar Higgs particle in scattering processes, unitarity is restored in the dynamical theory at high energies through the non-perturbative strong interactions between the particles. Since the longitudinal gauge field components are equivalent to the Goldstone fields in the microscopic theory, their strong interactions at high energies are transferred to the electroweak gauge bosons. Since, by unitarity, the S-wave scattering amplitude of longitudinally polarized W, Z bosons in the isoscalar channel $a_0^0 = \sqrt{2} G_{\mathrm{F}} s/16\pi$, is bound by $1/2$, the characteristic scale of the new strong interactions must be close to 1.2 TeV. Thus near the critial energy of 1 TeV the W, Z bosons interact strongly with each other. Technicolor theories provide a possible frame for such scenarios.

4.1. Dynamical symmetry breaking

Physical scenarios of dynamical symmetry breaking are based on new strong interaction theories, which extend the constituent spectrum and the interactions of the Standard Model. If these interactions are invariant under transformations of the chiral SU(2)×SU(2) group, for instance, the chiral invariance may be broken spontaneously down to the diagonal isospin group SU(2). This process is associated with the formation of a chiral condensate in the ground state and the existence of three massless Goldstone bosons.

The Goldstone bosons can be absorbed by the gauge fields, generating longitudinal states and non-zero masses. Summing up the geometric series of vector boson–Goldstone boson transitions in the propagator results in a shift of the mass pole:

$$\begin{aligned}\frac{1}{q^2} &\to \frac{1}{q^2} + \frac{1}{q^2} q_\mu \frac{g^2 F^2/2}{q^2} q_\mu \frac{1}{q^2} + \frac{1}{q^2}\left[\frac{g^2 F^2}{2}\frac{1}{q^2}\right]^2 + \cdots \\ &\to \frac{1}{q^2 - M^2}\,. \end{aligned} \tag{49}$$

The coupling between gauge fields and Goldstone bosons has been defined as $igF/\sqrt{2} q_\mu$. The mass of the gauge field is related to this coupling by

$$M^2 = \frac{1}{2} g^2 F^2\,. \tag{50}$$

The value of the coupling F must coincide numerically with $v/\sqrt{2} = 174$ GeV. The remaining custodial SU(2) symmetry guarantees that the ρ parameter, the relative strength between NC and CC couplings, is one.

Since the wave functions of longitudinally polarized vector bosons grow with the energy, the longitudinal field components are the dominant degrees of freedom at high energies. These states however can asymptotically be identified with the absorbed Goldstone bosons. The dynamics of gauge bosons can therefore be identified at high energies with the dynamics of scalar Goldstone fields. An elegant representation of the Goldstone fields is provided by the exponentiated form

$$U = \exp\left[\frac{-i\vec{\omega}\vec{\tau}}{v}\right] \tag{51}$$

which corresponds to an SU(2) matrix field.

In this scenario the Lagrangean of the system consists of the Yang–Mills part $\mathcal{L}_{\mathrm{YM}}$ and the interactions $\mathcal{L}_{\mathrm{G}}$ of the Goldstone fields, $\mathcal{L} = \mathcal{L}_{\mathrm{YM}} + \mathcal{L}_{\mathrm{G}}$. The Yang–Mills part is written in the usual form $\mathcal{L}_{\mathrm{YM}} = -\frac{1}{4}\mathrm{Tr}[W_{\mu\nu}W_{\mu\nu} + B_{\mu\nu}B_{\mu\nu}]$. The interactions of the Goldstone fields can be expanded in chiral theories systematically in the derivatives of the fields, corresponding to expansions in powers of energy for scattering amplitudes [62]:

$$\mathcal{L}_{\mathrm{G}} = \mathcal{L}_0 + \sum_{\mathrm{dim}=4} \mathcal{L}_i + \cdots . \tag{52}$$

Denoting the SM covariant derivative of the Goldstone fields by $D_\mu U = \partial_\mu U - igW_\mu U + ig'B_\mu U$ the leading term $\mathcal{L}_0$ of dimension $= 2$ is given by

$$\mathcal{L}_0 = \frac{v^2}{4}\mathrm{Tr}[D_\mu U^+ D_\mu U]\,. \tag{53}$$

This term generates the masses of W, Z gauge bosons: $M_W^2 = \frac{1}{4}g^2v^2$ and $M_Z^2 = \frac{1}{4}(g^2 + g'^2)v^2$. The only parameter in this part of the interactions is v which however is fixed uniquely by the experimental value of the W mass; thus the amplitudes predicted by the leading term in the chiral expansion can be considered parameter-free.

The next-to-leading term in the expansion with dimension $= 4$ consists of ten terms. If the custodial SU(2) symmetry is imposed, only two terms are found which do not affect propagators and 3-boson vertices but only 4-boson vertices *etc.* Introducing the vector field V_μ by $V_\mu = U^+ D_\mu U$, these two terms are given by the interaction densities

$$\begin{aligned} \mathcal{L}_4 &= \alpha_4 \left[\mathrm{Tr}V_\mu V_\nu\right]^2 , \\ \mathcal{L}_5 &= \alpha_5 \left[\mathrm{Tr}V_\mu V_\mu\right]^2 . \end{aligned} \tag{54}$$

The two coefficients α_4, α_5 are free parameters which must be adjusted experimentally from WW scattering data.

Higher orders in the chiral expansion give rise to an energy expansion of the scattering amplitudes of the form $\mathcal{A} = \sum c_n (s/v^2)^n$. This series will diverge for energies at which the resonances of the new strong interaction theory can be formed in WW collisions: 0^+ "Higgs-like", 1^- "ρ-like" resonances *etc.* The masses of these resonance states are expected in the range $M_{\rm R} \sim 4\pi v$ where chiral loop expansions diverge, *i.e.* between about 1 and 3 TeV.

4.2. WW scattering at high-energy colliders

The (quasi-)elastic 2–2 WW scattering amplitudes can be expressed at high energies by a master amplitude $A(s,t,u)$ which depends on the three Mandelstam variables of these processes:

$$\begin{aligned} A(W^+W^- \to ZZ) &= A(s,t,u)\,, \\ A(W^+W^- \to W^+W^-) &= A(s,t,u) + A(t,s,u)\,, \\ A(ZZ \to ZZ) &= A(s,t,u) + A(t,s,u) + A(u,s,t)\,, \\ A(W^-W^- \to W^-W^-) &= A(t,s,u) + A(u,s,t)\,. \end{aligned} \tag{55}$$

To lowest order in the chiral expansion, $\mathcal{L} \to \mathcal{L}_{\rm YM} + \mathcal{L}_0$, the master amplitude is given, in a parameter-free form, by the energy squared s:

$$A(s,t,u) \to \frac{s}{v^2}\,. \tag{56}$$

This representation is valid for energies $s \gg M_W^2$ but below the new resonance region, *i.e.* in practice at energies $\sqrt{s} = \mathcal{O}(1\ \text{TeV})$. Denoting the scattering length for the channel carrying isospin I and angular momentum J by a_{IJ}, the only non-zero scattering channels predicted by the leading term of the chiral expansion, correspond to

$$\begin{aligned} a_{00} &= +\frac{s}{16\pi v^2}\,, \qquad & a_{20} &= -\frac{s}{32\pi v^2}\,, \\ a_{11} &= +\frac{s}{96\pi v^2}\,. \end{aligned} \tag{57}$$

While the exotic $I = 2$ channel is repulsive, the $I = J = 0$ and $I = J = 1$ channels are attractive, indicating the formation of non-fundamental Higgs-type and ρ-type resonances.

Taking into account the next-to-leading terms in the chiral expansion, the master amplitude turns out to be [17]

$$A(s,t,u) = \frac{s}{v^2} + \alpha_4 \frac{4(t^2+u^2)}{v^4} + \alpha_5 \frac{8s^2}{v^4} + \cdots \tag{58}$$

including the two parameters α_4 and α_5.

Increasing the energy in the expansion, the amplitudes will approach the resonance area. In this area, the chiral character of the theory does not provide any more the guiding principle for the construction of the scattering amplitudes. Instead, *ad-hoc* hypotheses must be introduced to define the nature of the resonances; see *e.g.* Ref. [18].

e^+e^- linear colliders are excellent tools to study WW scattering. At high energies, equivalent W beams accompany the electron/positron beams in the fragmentation processes $ee \to \nu\nu WW$. In the hadronic LHC environment the final state W bosons can only be observed in leptonic decays. Resonance reconstruction is thus not possible for charged W final states. However, the clean environment of e^+e^- colliders will allow the reconstruction of resonances from W decays to jet pairs. The results of three experimental simulations are displayed in Fig. 18. In Fig. 18(a) the sensitivity to the parameters α_4, α_5 of the chiral expansion is shown for WW scattering in e^+e^- colliders [17]. The results of this analysis can be reinterpreted as sensitivity to the parameter-free prediction of the chiral expansion, corresponding to an error of about 10% in the first term of the master amplitude s/v^2. These experiments test the basic concept of dynamical symmetry breaking through spontaneous symmetry breaking. The production of a vector-boson resonance of mass $M_V = 1$ TeV is exemplified in [18] Fig.18(b).

A second powerful method measures elastic $W^+W^- \to W^+W^-$ scattering in the $I = 1, J = 1$ channel. The rescattering of W^+W^- bosons produced in e^+e^- annihilation depends at high energies on the WW scattering phase δ_{11} [63]. The production amplitude $F = F_{\mathrm{LO}} \times \mathcal{R}$ is the product of the lowest-order perturbative diagram with the Mushkelishvili-Omnès rescattering amplitude $\mathcal{R}$,

$$\mathcal{R} = \exp \frac{s}{\pi} \int \frac{ds'}{s'} \frac{\delta_{11}(s')}{s' - s - i\varepsilon} \tag{59}$$

which is determined by the $I = J = 1$ WW phase shift δ_{11}. The power of this method derives from the fact that the entire energy of the e^+e^- collider is transferred to the WW system [while a major fraction of the energy is lost in the fragmentation of $e \to \nu W$ when WW scattering is studied in the process $ee \to \nu\nu WW$]. Detailed simulations [64] have shown that this process is sensitive to vector-boson masses up to about $M_V \lesssim 6$ TeV.

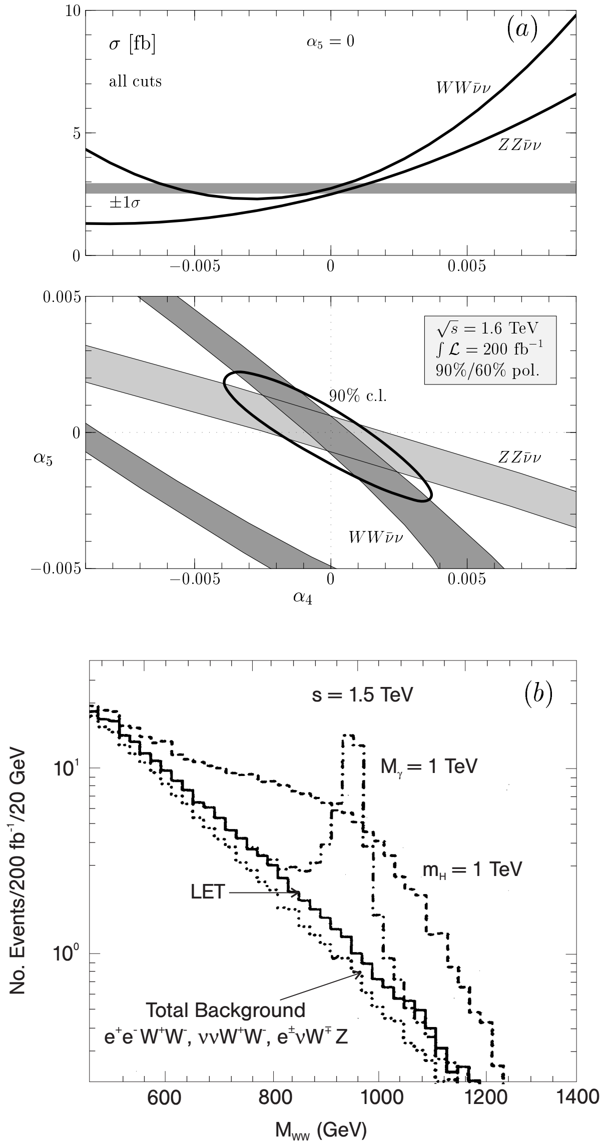

Fig. 18. Upper part: Sensitivity to the expansion parameters in chiral electroweak models of $WW \to WW$ and $WW \to ZZ$ scattering at the strong-interaction threshold; Ref. [17]. Lower part: The distribution of the WW invariant energy in $e^+e^- \to \overline{\nu}\nu WW$ for scalar and vector resonance models $[M_H, M_V = 1$ TeV], as well as for non-resonant WW scattering in chiral models near the threshold; Ref. [18].

5. Summary

The mechanism of electroweak symmetry breaking can be established in the present and the next generation of e^+e^- colliders when operated at high luminosities:

- ⋆ It can be proved unambiguously whether a light fundamental Higgs boson does exist;
- ⋆ The profile of the particle can be reconstructed, which reveals the physical nature of the underlying mechanism of electroweak symmetry breaking;
- ⋆ Analyses of strong WW scattering can be performed if the symmetry breaking is of dynamical nature and generated in a novel strong interaction theory.

Moreover, depending on the ultimate experimental answer to these questions, the electroweak sector will provide the platform for extrapolations into physical areas beyond the Standard Model: either to a low-energy supersymmetry sector at a scale less than about 1 TeV or, alternatively, to a new strong interaction theory at a characteristic scale of order 1 TeV.

First of all, I should like to thank very warmly the organisers for the invitation to the 1999 Kraków Epiphany Conference. Moreover, I am very grateful to M. Mühlleitner and M. Spira for the collaboration on material presented in this report. Thanks go also to S. Günther and M. Maniatis for LaTeXing the manuscript.

REFERENCES

[1] P.W. Higgs, *Phys. Rev. Lett.* **12**, 132 (1964); *Phys. Rev.* **145**, 1156 (1966); F. Englert, R. Brout, *Phys. Rev. Lett.* **13**, 321 (1964); G.S. Guralnik, C.R. Hagen, T.W. Kibble, *Phys. Rev. Lett.* **13**, 585 (1964).

[2] S. Weinberg, *Phys. Rev.* **D13**, 974 (1979); *Phys. Rev.* **D19**, 1277 (1979); L. Susskind, *Phys. Rev.* **D20**, 2619 (1979).

[3] S.L. Glashow, *Nucl. Phys.* **20**, 579 (1961); S. Weinberg, *Phys. Rev. Lett.* **19**, 1264 (1967); A. Salam, in *Elementary Particle Theory*, ed. N. Svartholm, Almqvist and Wiksells, Stockholm 1968.

[4] N. Cabibbo, L. Maiani, G. Parisi, R. Petronzio, *Nucl. Phys.* **B158**, 295 (1979); R.A. Flores, M. Sher, *Phys. Rev.* **D27**, 1679 (1983); M. Lindner, *Z. Phys.* **C31**, 295 (1986); M. Sher, *Phys. Rep.* **179**, 273 (1989); J. Casas, J. Espinosa, M. Quiros, *Phys. Lett.* **B342**, 171 (1995).

[5] G. Altarelli, G. Isidori, *Phys. Lett.* **B337**, 141 (1994); J. Espinosa, M. Quiros, *Phys. Lett.* **B353**, 257 (1995).

[6] A. Hasenfratz, K. Jansen, C. Lang, T. Neuhaus, H. Yoneyama, *Phys. Lett.* **B199**, 531 (1987); J. Kuti, L. Liu, Y. Shen, *Phys. Rev. Lett.* **61**, 678 (1988); M. Lüscher, P. Weisz, *Nucl. Phys.* **B318**, 705 (1989).

[7] M. Veltman, *Acta Phys. Pol.* **B8**, 475 (1977).

[8] LEP Electroweak Working Group, Report CERN–EP/99–15.

[9] Experimental reports to the LEPC meeting, CERN November 1998.

[10] E. Accomando *et al., Phys. Rep.* **299**, 1 (1998).

[11] P. Fayet, S. Ferrara, *Phys. Rep.* **32**, 249 (1977); H.P. Nilles, *Phys. Rep.* **110**, 1 (1984); H. Haber, G. Kane, *Phys. Rep.* **117**, 75 (1985); R. Barbieri, *Riv. Nuovo Cim.* **11**, 1 (1988).

[12] E. Witten, *Phys. Lett.* **B105**, 267 (1981).

[13] L.E. Ibañez, G.G. Ross, *Phys. Lett.* **B105**, 439 (1981); S. Dimopoulos, S. Raby, F. Wilczek, *Phys. Rev.* **D24**, 1681 (1981); J. Ellis, S. Kelley, D.V. Nanapoulos, *Phys. Lett.* **B249**, 441 (1990); P. Langacker, M. Luo, *Phys. Rev.* **D44**, 817 (1991); U. Amaldi, W. de Boer, H. Fürstenau, *Phys. Lett.* **B260**, 447 (1991).

[14] K. Inonue, A. Kakuto, H. Komatsu, S. Takeshita, *Prog. Theor. Phys.* **67**, 1889 (1982); R. Flores, M. Sher, *Ann. Phys.* **148**, 95 (1983); H.P. Nilles, M. Nusbaumer, *Phys. Lett.* **B145**, 73 (1984); P. Majumdar, P. Roy, *Phys. Rev.* **D30**, 2432 (1984).

[15] J.F. Gunion, H.E. Haber, *Nucl. Phys.* **B272**, 1 (1986); **B278**, 449 (1986).

[16] S. Dawson, *Nucl. Phys.* **B249**, 42 (1985); M. Chanowitz, M.K. Gaillard, *Phys. Lett.* **B142**, 85 (1984); G. Kane, W. Repko, W. Rolnick, *Phys. Lett.* **B148**, 367 (1984).

[17] E. Boos, H.-J. He, W. Kilian, A. Pukhov, C.-P. Yuan, P.M. Zerwas, *Phys. Rev.* **D57**, 1553 (1998).

[18] V. Barger, K. Cheung, T. Han, R.J.N. Phillips, *Phys. Rev.* **D52**, 3815 (1995).

[19] J.F. Gunion, H.E. Haber, G. Kane, S. Dawson, *The Higgs Hunter's Guide*, Addison–Wesley, 1990; *Perspectives on Higgs Physics*, ed. G.L. Kane, World Scientific, 1993; A. Dobado, A. Gómez-Nicola, A.L. Maroto, J.R. Peláez, *Effective Lagrangians for the Standard Model*, Springer, 1997.

[20] M. Spira, P.M. Zerwas, in Proceedings of the 36. Internationale Universitätswoche für Kern- und Teilchenphysik, Schladming 1997.

[21] B.W. Lee, C. Quigg, H.B. Thacker, *Phys. Rev. Lett.* **38**, 883 (1977).

[22] E. Braaten, J.P. Leveille, *Phys. Rev.* **D22**, 715 (1980); N. Sakai, *Phys. Rev.* **D22**, 2220 (1980); T. Inami, T. Kubota, *Nucl. Phys.* **B179**, 171 (1981); S.G. Gorishny, A.L. Kataev, S.A. Larin, *Sov. J. Nucl. Phys.* **40**, 329 (1984); M. Drees, K. Hikasa, *Phys. Rev.* **D41**, 1547 (1990); *Phys. Lett.* **B240**, 455 (1990) and (E) **B262**, 497 (1991);

[23] B.A. Kniehl, *Nucl. Phys.* **B352**, 1 (1991); *Nucl. Phys.* **B357**, 357 (1991); D.Yu. Bardin, B.M. Vilenskiĭ, P.Kh. Khristova, Report JINR-P2-91-140.

[24] T.G. Rizzo, *Phys. Rev.* **D22**, 389 (1980); W.-Y. Keung, W.J. Marciano, *Phys. Rev.* **D30**, 248 (1984).

[25] A. Djouadi, M. Spira, P.M. Zerwas, *Phys. Lett.* **B264**, 440 (1991); M. Spira, A. Djouadi, D. Graudenz, P.M. Zerwas, *Nucl. Phys.* **B453**, 17 (1995).

[26] J. Ellis, M.K. Gaillard, D.V. Nanopoulos, *Nucl. Phys.* **B106**, 292 (1976).

[27] A. Blondel, *Acta Phys. Pol.* **B30**, 1851 (1999).

[28] B.L. Ioffe, V.A. Khoze, *Sov. J. Part. Nucl.* **9**, 50 (1978).

[29] B.W. Lee, C. Quigg, H.B. Thacker, *Phys. Rev.* **D16**, 1519 (1977).

[30] R.N. Cahn, S. Dawson, *Phys. Lett.* **B136**, 96 (1984); G.L. Kane, W.W. Repko, W.B. Rolnick, *Phys. Lett.* **B148**, 367 (1984); G. Altarelli, B. Mele, F. Pitolli, *Nucl. Phys.* **B287**, 205 (1987); W. Kilian, M. Krämer, P.M. Zerwas, *Phys. Lett.* **B373**, 135 (1996).

[31] H.J Schreiber *et al.*, in: DESY–ECFA Conceptual LC Design Report (1997).

[32] D.L. Borden, D.A. Bauer, D.O. Caldwell, *Phys. Rev.* **D48**, 4018 (1993); G. Jikia, *Nucl. Phys.* **B405**, 24 (1993).

[33] I.F. Ginzburg, G.L. Kotkin, S.L. Panfil, V.G. Serbo, V.I. Telnov, *Nucl. Instrum. Methods Phys. Rep.* **219**, 5 (1984).

[34] P. Janot, Proceedings *Physics and Experiments with e^+e^- Linear Colliders*, Waikoloa/Hawaii 1993, eds. F. Harris, S. Olsen, S. Pakvasa and X. Tata, World Scientific 1993.

[35] V. Barger, K. Cheung, A. Djouadi, B.A. Kniehl, P. Zerwas, *Phys. Rev.* **D49**, 79 (1994).

[36] M. Hildreth, T. Barklow, D. Burke, *Phys. Rev.* **D49**, 3441 (1994); M. Battaglia *et al.*, in: DESY–ECFA Conceptual LC Design Report (1997).

[37] A. Djouadi, J. Kalinowski, P.M. Zerwas, *Mod. Phys. Lett.* **A7**, 1765 (1992); *Z. Phys.* **C54**, 255 (1992); M. Dittmaier, M. Krämer, Y. Liao, M. Spira, P.M. Zerwas, *Phys. Lett.* **B441**, 383 (1998).

[38] T. Matsui, *Acta Phys. Pol.* **B30**, 2041 (1999).

[39] K. Hagiwara, H. Murayama, I. Watanabe, *Nucl. Phys.* **B367**, 257 (1991).

[40] A. Djouadi, W. Kilian, M. Mühlleitner, P.M. Zerwas, Report DESY 99-001 [hep-ph/9903288]; *Eur. Phys. J.* **C** in press.

[41] J. Polchinski, L. Susskind, *Phys. Rev.* **D26**, 3661(1982); S. Dimopoulos, H. Georgi, *Nucl. Phys.* **B193**, 150 (1981); N. Sakai, *Z. Phys.* **C11**, 153 (1981).

[42] L.E. Ibañez, G.G. Ross, *Phys. Lett.* **B110**, 215 (1982).

[43] Y. Okada, M. Yamaguchi, T. Yanagida, *Progr. Theor. Phys.* **85**, 1 (1991); H. Haber, R. Hempfling, *Phys. Lett.* **66**, 1815 (1991); J. Ellis, G. Ridolfi, F. Zwirner, *Phys. Lett.* **257B**, 83 (1991); M. Carena, J.R. Espinosa, M. Quiros, C.E.M. Wagner, *Phys. Lett.* **B335**, 209 (1995); S. Heinemeyer, W. Hollik, G. Weiglein, KA-TP-17-1998.

[44] M. Carena, S. Pokorski, C. Wagner, *Nucl. Phys.* **B406**, 59 (1993); V. Barger, M.S. Berger, P. Ohmann, *Phys. Rev.* **D47**, 1093 (1993).

[45] A. Djouadi, J. Kalinowski, P.M. Zerwas, *Z. Phys.* **C70**, 435 (1996).

[46] A. Djouadi, P. Janot, J. Kalinowski, P.M. Zerwas, *Phys. Lett.* **B376**, 220 (1996).

[47] A. Djouadi, J. Kalinowski, P. Ohmann, P.M. Zerwas, DESY 95-213 and *Z. Phys.* **C74**, 93 (1997).

[48] A. Bartl, H. Eberl, K. Hidaka, T. Kon, W. Majerotto, Y. Yamada, *Phys. Lett.* **B389**, 538 (1996).

[49] A. Djouadi, J. Kalinowski, P.M. Zerwas, *Z. Phys.* **C57**, 569 (1993).

[50] P. Janot, Proceedings, *Physics and Experiments with* e^+e^- *Linear Colliders, Waikoloa/Hawaii 1993*, eds. F. Harris, S. Olsen, S. Pakvasa and X. Tata, World Scientific 1993.

[51] A. Andreazza, C. Troncon, in: DESY–ECFA Conceptual LC Design Report (1997).

[52] A. Sopczak, *Z. Phys.* **C65**, 449 (1995).

[53] A. Djouadi, H.E. Haber, P.M. Zerwas, *Phys. Lett.* **B375**, 203 (1996).

[54] P. Osland, P.N. Pandita, *Phys. Rev.* **D59**, 055013 (1999); P. Osland, *Acta Phys. Pol.* **B30**, 1967 (1999).

[55] M. Krämer, J. Kühn, M.L. Stong, P.M. Zerwas, *Z. Phys.* **C64**, 21 (1994).

[56] P. Fayet, *Nucl. Phys.* **B90**, 104 (1975); H.-P. Nilles, M. Srednicki, D. Wyler, *Phys. Lett.* **B120**, 346 (1983); J.-P. Derendinger, C.A. Savoy, *Nucl. Phys.* **B237**, 307 (1984); J.F. Gunion, H.E. Haber, *Nucl. Phys.* **B272**, 1 (1986); J. Ellis, J.F. Gunion, H.E. Haber, L. Roszkowski, F. Zwirner, *Phys. Rev.* **D39**, 844 (1989).

[57] U. Ellwanger, M. Rausch de Traubenberg, C.A. Savoy, *Z. Phys.* **C67**, 665 (1995); S.F. King, P.L. White, *Phys. Rev.* **D52**, 4183 (1995); H. Asatrian, K. Eguin, *Mod. Phys. Lett.* **A10**, 2943 (1995).

[58] J.R. Espinosa, M. Quiros, *Phys. Lett.* **B279**, 92 (1992); G.L. Kane, C. Kolda, J.D. Wells, *Phys. Rev. Lett.* **70**, 2686 (1993).

[59] M. Carena, P.M. Zerwas (*conv.*) *et al.*, *Higgs Physics at LEP2*, CERN Report 96–01 [hep-ph/9602250], G. Altarelli, T. Sjöstrand and F. Zwirner (eds.).

[60] J. Kamoshita, Y. Okada, M. Tanaka, *Phys. Lett.* **B328**, 67 (1994).

[61] J.M. Cornwall, D.N. Levin, G. Tiktopoulos, *Phys. Rev.* **D10**, 1145 (1974); B. Lee, C. Quigg, H. Thacker, *Phys. Rev.* **D16**, 1519 (1977); M. Chanowitz, M.K. Gaillard, *Nucl. Phys.* **B261**, 379 (1985); G.J. Gounaris, R. Kogerler, H. Neufeld, *Phys. Rev.* **D34**, 3257 (1986); Y.P. Yao, C.P. Yuan, *Phys. Rev.* **D38**, 2237 (1988); H.-J. He, Y.-P. Kuang, X.-Y. Li, *Phys. Rev. Lett.* **69**, 2619 (1992).

[62] T. Appelquist, C. Bernard, *Phys. Rev.* **D22**, 200 (1980); A. Longhitano, *Phys. Rev.* **D22**, 1166 (1980); *Nucl. Phys.* **B188**, 118 (1981); T. Appelquist, G.-H. Wu, *Phys. Rev.* **D48**, 3235 (1993).

[63] M.E. Peskin, Proceedings, *Physics and Experiments with Linear Colliders*, Saariselkä 1991.

[64] T.L. Barklow, DPF Conference, Albuquerque (1994).